their proliferation (Fig. 3A). By contrast, overexpression of PCDH10 did not affect proliferation of T98G or U251 cells, which do not express detectable levels of PCDH10 protein (Supplementary Fig. 2). We also performed AnnexinV assays and found that knockdown of PCDH10 induced apoptosis of GB2 cells (Fig. 3B and C). We next performed sphere formation assays to clarify the role of PCDH10 in the self-renewal capacity of glioblastoma cells. We found that knockdown of PCDH10 by shRNA resulted in significant inhibition of sphere formation (Fig. 3D and E). Thus, PCDH10 may be critical for the proliferation, survival and self-renewal of glioblastoma cells.

3.4. Knockdown of PCDH10 suppresses the tumorigenicity of glioblastoma cells

To clarify the role of PCDH10 in the tumorigenicity of glioblastoma cells, we orthotopically transplanted GB16 cells that had been infected with a lentivirus expressing GFP and an shRNA targeting PCDH10 into the frontal lobe of nude mice. We found that the mice transplanted with PCDH10-knockdown GB16 cells survived longer than control mice (sh PCDH10#2, log-rank test $p = 0.042$; sh PCDH10#4, log-rank test $p = 0.00031$) (Fig. 4A). Histological studies revealed that all mice transplanted with

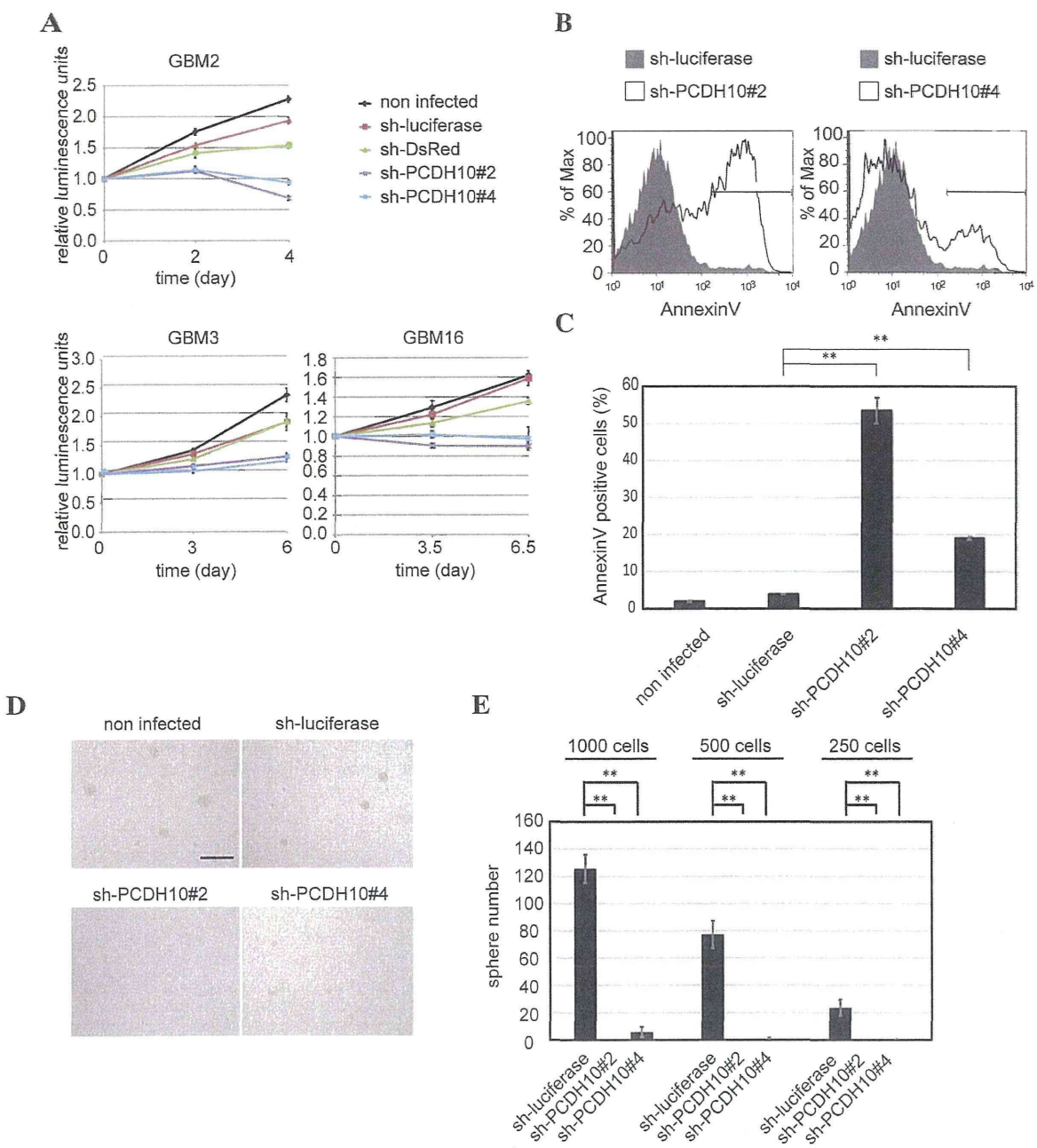

Fig. 3. PCDH10 is required for the proliferation, survival and self-renewal of glioblastoma cells. (A) Cell Titer-Glo assays were performed with GB2, GB3 or GB16 cells infected with a lentivirus expressing an shRNA targeting PCDH10 (MOI = 3). Results are shown as average of 5 wells ± SD. (B) AnnexinV assays were performed with GB2 cells that had been infected with a lentivirus expressing an shRNA targeting PCDH10 for 8 days. (C) AnnexinV-positive populations in (B) are shown. Results are shown as the mean ± SD ($n = 3$). At least 5000 cells were analyzed per sample. $^{**}p < 0.01$. (D and E) Sphere formation assays were performed with GB2 cells that had been infected with a lentivirus expressing an shRNA targeting PCDH10 for 17 days. (D) Bright field images of spheres. (E) Results are shown as average of 6 wells ± SD. $^{**}p < 0.01$.

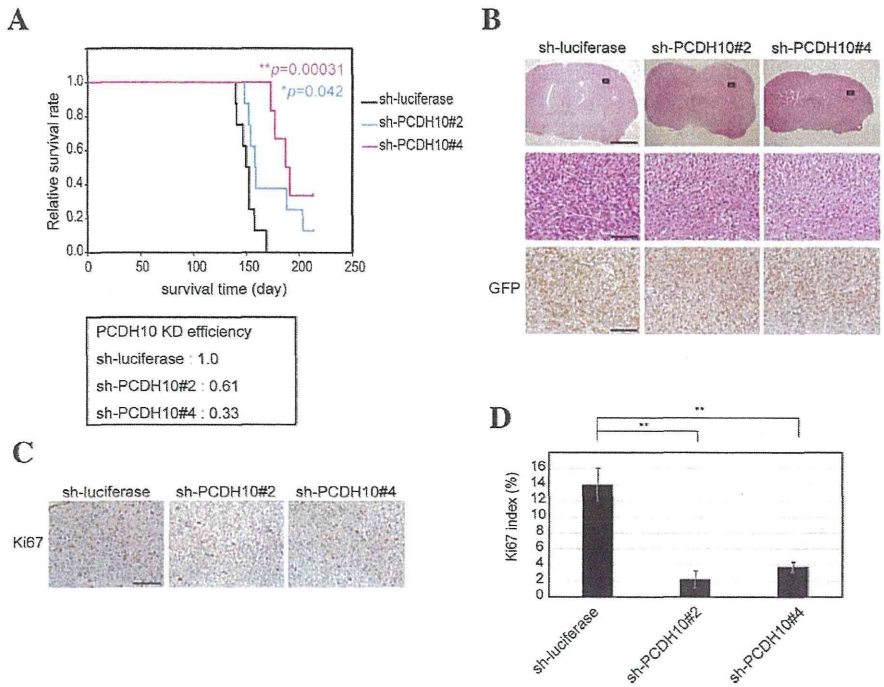

Fig. 4. PCDH10 is required for the tumorigenicity of glioblastoma cells. (A) Kaplan–Meier survival curves of mice transplanted with 1.0×10^4 GB16 cells infected with a lentivirus expressing GFP and shRNA targeting PCDH10 or luciferase (control) (MOI = 1; $n = 8$ for shPCDH10#2 and luciferase; $n = 6$ for shPCDH10#4). (B) Histological analysis of tumors harvested from the mice in (A). Tissue sections were stained with HE or anti-GFP antibody. General views (Upper Panel; Scale bar, 2.0 mm) and magnified views (Middle and Lower panels; Scale bars, 100 μm) of the region around the corpus callosum in the right hemisphere (near the injection point, black squares in the upper panel). (C and D) Immunohistochemical analysis of tumors harvested from the mice in (A). Tissue sections were stained with anti-GFP and anti-Ki-67 antibodies. Scale bars, 100 μm. (D) Ki67 indices of the brain sections. 1.0×10^3 cells were counted in each field. Results are shown as average of 6 fields ± SD. $^{**}p < 0.01$.

GB16 cells had developed tumors with diffuse infiltration into surrounding brain tissues, one of the hallmark features of glioblastoma (Fig. 4B). The density of GFP-expressing cells (injected tumor cells) was slightly lower in the brains of the mice transplanted with PCDH10-knockdown GB16 cells compared to those of control mice (Fig. 4B). Furthermore, we observed that the number of Ki67-positive cells was significantly reduced in the brains of the mice transplanted with PCDH10-knockdown GB16 cells compared to those of control mice (sh-luciferase, 14.0 ± 2.0%; sh-PCDH10#2, 2.2 ± 1.1%; sh-PCDH10#4, 3.7 ± 0.64%) (Fig. 4C and D). These results suggest that knockdown of PCDH10 suppresses the proliferation of glioblastoma cells and extends the survival of tumor-bearing mice.

These results show that PCDH10 is required for the proliferation and tumorigenicity of glioblastoma cells. This suggests that PCDH10 may function differently at the molecular level in glioblastoma cells compared to other tumor cell types. This may mean that PCDH10 associates with different molecules and elicits different downstream signals in glioblastoma cells than it does in other tumor cells. The molecular mechanisms underlying this functional difference remain to be elucidated. It also remains to be investigated whether PCDH10 expression levels are associated with the classification and prognosis of glioblastoma patients. Finally, we speculate that PCDH10 may be a potential therapeutic target for glioblastoma. In particular, monoclonal antibodies that target the extracellular domain of PCDH10 could hold promise as novel anti-tumor reagents.

Acknowledgments

This work was supported by Research Program of Innovative Cell Biology by Innovative Technology (Integrated Systems Analysis of Cellular Oncogenic Signaling Networks), Grants-in-Aid for Scientific Research on Innovative Areas (Integrative Research on Cancer Microenvironment Network), Project for Development of Innovative Research on Cancer Therapeutics, Grant-in-Aid for Scientific Research (C-23592117) from the Japan Society for the Promotion of Science (M. Nakada) and Foundation for Promotion of Cancer Research (M. Nakada), Takeda Science Foundation, Kato Memorial Bioscience Foundation and in part by Global COE Program (Integrative Life Science Based on the Study of Biosignaling Mechanisms), MEXT, Japan.

Appendix A. Supplementary data

Supplementary data associated with this article can be found, in the online version, at http://dx.doi.org/10.1016/j.bbrc.2013.12.138.

References

[1] Q. Wu, T. Maniatis, A striking organization of a large family of human neural cadherin-like cell adhesion genes, Cell 97 (1999) 779–790.
[2] S. Hirano, M. Takeichi, Cadherins in brain morphogenesis and wiring, Physiol. Rev. 92 (2011) 597–634.
[3] W.V. Chen, T. Maniatis, Clustered protocadherins, Development 140 (2013) 3297–3302.
[4] S. Hirano, Q. Yan, S.T. Suzuki, Expression of a novel protocadherin, OL-protocadherin, in a subset of functional systems of the developing mouse brain, J. Neurosci. 19 (1999) 995–1005.
[5] S. Nakao, A. Platek, S. Hirano, M. Takeichi, Contact-dependent promotion of cell migration by the OL-protocadherin-Nap1 interaction, J. Cell Biol. 182 (2008) 395–410.
[6] M. Uemura, S. Nakao, S.T. Suzuki, M. Takeichi, S. Hirano, OL-protocadherin is essential for growth of striatal axons and thalamocortical projections, Nat. Neurosci. 10 (2007) 1151–1159.
[7] K. Miyamoto, T. Fukutomi, S. Akashi-Tanaka, T. Hasegawa, T. Asahara, T. Sugimura, T. Ushijima, Identification of 20 genes aberrantly methylated in human breast cancers, Int. J. Cancer 116 (2005) 407–414.
[8] J. Ying, H. Li, T.J. Seng, C. Langford, G. Srivastava, S.W. Tsao, T. Putti, P. Murray, A.T. Chan, Q. Tao, Functional epigenetics identifies a protocadherin PCDH10 as a candidate tumor suppressor for nasopharyngeal, esophageal and multiple other carcinomas with frequent methylation, Oncogene 25 (2006) 1070–1080.

[9] X. Zhong, Y. Zhu, J. Mao, J. Zhang, S. Zheng, Frequent epigenetic silencing of PCDH10 by methylation in human colorectal cancer, J. Cancer Res. Clin. Oncol. 139 (2013) 485–490.
[10] J. Ying, Z. Gao, H. Li, G. Srivastava, P.G. Murray, H.K. Goh, C.Y. Lim, Y. Wang, T. Marafioti, D.Y. Mason, R.F. Ambinder, A.T. Chan, Q. Tao, Frequent epigenetic silencing of protocadherin 10 by methylation in multiple haematologic malignancies, Br. J. Haematol. 136 (2007) 829–832.
[11] J. Yu, Y.Y. Cheng, Q. Tao, K.F. Cheung, C.N. Lam, H. Geng, L.W. Tian, Y.P. Wong, J.H. Tong, J.M. Ying, H. Jin, K.F. To, F.K. Chan, J.J. Sung, Methylation of protocadherin 10, a novel tumor suppressor, is associated with poor prognosis in patients with gastric cancer, Gastroenterology 136 (2009). 640–651 e641.
[12] J.G. Ma, Z.K. He, J.H. Ma, W.P. Li, G. Sun, Downregulation of protocadherin-10 expression correlates with malignant behaviour and poor prognosis in human bladder cancer, J. Int. Med. Res. 41 (2013) 38–47.
[13] J. Chen, R.M. McKay, L.F. Parada, Malignant glioma: lessons from genomics, mouse models, and stem cells, Cell 149 (2012) 36–47.
[14] R. Koyama-Nasu, Y. Nasu-Nishimura, T. Todo, Y. Ino, N. Saito, H. Aburatani, K. Funato, K. Echizen, H. Sugano, R. Haruta, M. Matsui, R. Takahashi, E. Manabe, T. Oda, T. Akiyama, The critical role of cyclin D2 in cell cycle progression and tumorigenicity of glioblastoma stem cells, Oncogene 32 (2013) 3840–3845.
[15] J. Lee, S. Kotliarova, Y. Kotliarov, A. Li, Q. Su, N.M. Donin, S. Pastorino, B.W. Purow, N. Christopher, W. Zhang, J.K. Park, H.A. Fine, Tumor stem cells derived from glioblastomas cultured in bFGF and EGF more closely mirror the phenotype and genotype of primary tumors than do serum-cultured cell lines, Cancer Cell 9 (2006) 391–403.
[16] S.M. Pollard, K. Yoshikawa, I.D. Clarke, D. Danovi, S. Stricker, R. Russell, J. Bayani, R. Head, M. Lee, M. Bernstein, J.A. Squire, A. Smith, P. Dirks, Glioma stem cell lines expanded in adherent culture have tumor-specific phenotypes and are suitable for chemical and genetic screens, Cell Stem Cell 4 (2009) 568–580.
[17] M. Nakada, S. Nakada, T. Demuth, N.L. Tran, D.B. Hoelzinger, M.E. Berens, Molecular targets of glioma invasion, Cell. Mol. Life Sci. 64 (2007) 458–478.

Oncogene (2013), 1–9

www.nature.com/onc

ORIGINAL ARTICLE

The pleiotrophin-ALK axis is required for tumorigenicity of glioblastoma stem cells

R Koyama-Nasu[1], R Haruta[1], Y Nasu-Nishimura[1], K Taniue[1], Y Katou[2], K Shirahige[2], T Todo[3], Y Ino[3], A Mukasa[3], N Saito[3], M Matsui[1], R Takahashi[1], A Hoshino-Okubo[1], H Sugano[1], E Manabe[1], K Funato[1] and T Akiyama[1]

Increasing evidence suggests that brain tumors arise from the transformation of neural stem/precursor/progenitor cells. Much current research on human brain tumors is focused on the stem-like properties of glioblastoma. Here we show that anaplastic lymphoma kinase (ALK) and its ligand pleiotrophin are required for the self-renewal and tumorigenicity of glioblastoma stem cells (GSCs). Furthermore, we demonstrate that pleiotrophin is transactivated directly by SOX2, a transcription factor essential for the maintenance of both neural stem cells and GSCs. We speculate that the pleiotrophin-ALK axis may be a promising target for the therapy of glioblastoma.

Oncogene advance online publication, 20 May 2013; doi:10.1038/onc.2013.168

Keywords: ALK; cancer stem cell; glioblastoma; kinase; pleiotrophin; SOX2

INTRODUCTION

Glioblastoma is one of the most aggressive human cancers with a median survival of around 1 year.[1] Increasing evidence suggests that glioblastoma may arise from the transformation of neural stem/precursor/progenitor cells.[2] Consistent with this idea, glioblastoma cells cultured in serum-free media, which favor the growth of neural stem cells (NSCs), maintain stem-like properties and tumorigenicity.[3] However, when grown in the presence of serum, they undergo irreversible differentiation and lose their tumorigenicity.[3] This finding raises the possibility that differentiation therapy might be effective for glioblastoma.[4]

Almost all cell proliferative signaling involves phosphotransfer cascades, and accordingly protein kinases have been intensely pursued as drug targets. Indeed, a number of small-molecule inhibitors and antibodies targeting kinases are currently being used for cancer treatment.[5] Therefore, one approach to developing differentiation-inducing therapies for glioblastoma would be to identify kinases that regulate their stem-like properties.

Anaplastic lymphoma kinase (ALK) is a receptor tyrosine kinase that is bound by the growth factor pleiotrophin or the closely related midkine.[6,7] ALK was initially discovered as a protein fused to nucleophosmin (NPM) in an anaplastic large cell lymphoma (ALCL). This fusion was shown to cause the ligand-independent autophosphorylation and activation of ALK. Studies using mouse models further showed that this NPM-ALK fusion is a primary driver of oncogenesis in ALCL.[8] Moreover, oncogenic fusions or mutations of ALK have also been described in various other cancers, including inflammatory myofibroblastic tumors, non-small cell lung cancer (NSCLC), diffuse large B-cell lymphoma, squamous cell carcinoma of the esophagus and neuroblastoma.[7] Importantly, the ALK inhibitor crizotinib has recently been approved for the treatment of ALK-positive NSCLC.[9,10] In addition, an anti-ALK antibody has been shown to repress the invasive capacity of the glioblastoma cell line U87 (Stylianou *et al.*[11]).

The Sry-related transcription factor SOX2 was identified as a partner of Oct3/4 in embryonic stem cells (ESCs) and is known to be essential for pluripotent cell development.[12–14] SOX2 is also expressed in NSCs and has an important role in neural development and homeostasis of the adult central nervous system.[14,15] On the other hand, it has also been shown that SOX2 is overexpressed in glioblastoma.[16] Furthermore, it has been reported that knockdown of SOX2 by RNA interference (RNAi) suppresses the tumorigenicity of glioblastoma stem cells (GSCs) xenografted into immunodeficient mice.[17]

In the present study, we show that the pleiotrophin-ALK axis is activated by SOX2 and is required for the self-renewal and tumorigenicity of GSCs.

RESULTS

ALK and its ligand pleiotrophin are required for the self-renewal and stem-like properties of GSCs

We established four GSC lines under serum-free conditions, GB2–5, and found that they are of the proneural type.[18,19] These cell lines exhibited enrichment for GSCs as they maintained sphere-forming ability and expressed high levels of the NSC markers, SOX2 and Nestin, as reported previously[3] (Figure 1). The GB2 cell line possesses the highest tumorigenic activity among our GSC lines, and we used these cells to perform an unbiased kinome-wide RNAi screen. We transfected GB2 cells that had been maintained in serum-free medium with a library of small interference RNAs (siRNAs) that target each of 704 kinases and kinase-related genes and then measured the expression levels of the stem cell markers *CD133*[20] and *Lgr5*.[21] We found 15 kinase genes whose suppression affected *CD133* or *Lgr5* expression, including 4 kinases known to be involved in the proliferation of GSCs[22] (Table 1 and Supplementary Table S1). One of these top 15 genes, ALK was also previously reported to be involved in

[1]Laboratory of Molecular and Genetic Information, Institute of Molecular and Cellular Biosciences, The University of Tokyo, Bunkyo-ku, Tokyo, Japan; [2]Laboratory of Genome Structure and Function, Center for Epigenetic Disease, Institute of Molecular and Cellular Biosciences, The University of Tokyo, Bunkyo-ku, Tokyo, Japan and [3]Department of Neurosurgery, The University of Tokyo Hospital, Bunkyo-ku, Tokyo, Japan. Correspondence: Professor T Akiyama, Laboratory of Molecular and Genetic Information, Institute for Molecular and Cellular Bioscience, The University of Tokyo, Yayoi 1-1-1, Bunkyo-ku, Tokyo 113-0032, Japan.
E-mail: akiyama@iam.u-tokyo.ac.jp
Received 27 June 2012; revised 23 March 2013; accepted 25 March 2013

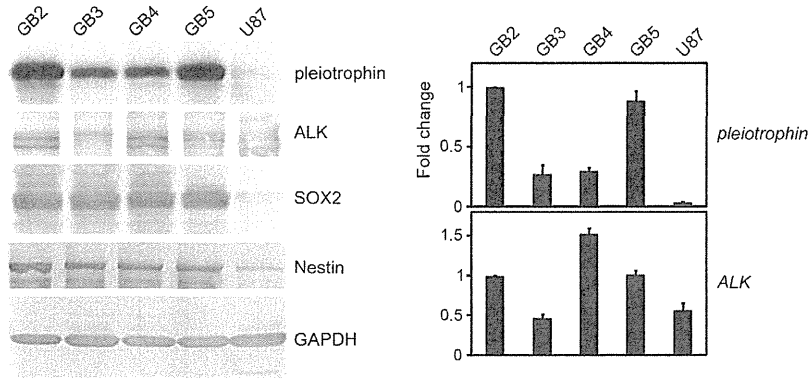

Figure 1. Expression levels of ALK and pleiotrophin in GSCs. GB2–5 cells were maintained in serum-free medium. U87 cells were maintained in serum-containing medium. Cell lysates were subjected to immunoblotting with antibodies to the indicated proteins (left). The mRNA levels of *ALK* or *pleiotrophin* were evaluated by quantitative RT–PCR and shown as the fold change over mRNA levels in GB2 cells (right). Error bars represent the s.d. ($n = 3$).

Table 1. Kinome-wide RNAi screen in GSCs

	Gene symbol	*CD133*	*Lgr5*	*Average*
1	TSSK6	0.55	0.50	0.52
2	GRK4	0.49	0.81	0.65
3	FRK	0.58	0.76	0.67
4	CDC42BPA*	0.45	0.89	0.67
5	PICK1	0.71	0.70	0.71
6	TAL1	0.78	0.64	0.71
7	DVL3	0.80	0.62	0.71
8	PCTK2	0.78	0.65	0.71
9	MARK1	0.70	0.73	0.72
10	OXSR1*	0.75	0.70	0.72
11	FYN*	0.53	0.91	0.72
12	DYRK2	0.76	0.70	0.73
13	MAPKAPK3*	0.68	0.80	0.74
14	**ALK**	**0.69**	**0.80**	**0.75**
15	ETNK2	0.89	0.60	0.75

Abbreviations: GSC, glioblastoma stem cell; RNAi, RNA interference. Note: Average fold changes in the top 15 genes whose knockdown resulted in the greatest change in CD133 and/or Lgr5 expression. ALK data are indicated in bold and the asterisks indicate genes identified in a similar RNAi screen.[22] The entire results are shown in Supplementary Table S1.

glioblastomagenesis.[11,23] However, these studies mainly analyzed the commonly used glioblastoma cell line U87, which does not exhibit any stem-like properties.[3,24] Furthermore, although U87 cells are highly tumorigenic, U87-derived tumors do not show any glioblastoma-specific features.[3,24] We therefore set out to study the role of ALK in the tumorigenicity of GSCs. Lentiviral introduction of a short hairpin RNA (shRNA) targeting ALK resulted in a decrease in both sphere formation and stem cell marker expression (Figures 2a and b). Although the levels of *nestin* mRNA were downregulated, the levels of Nestin protein did not change drastically, probably due to the stability of the Nestin protein in GB2 cells.

We next examined whether the ALK ligand pleiotrophin is required for the stem-like properties of GSCs. We found that pleiotrophin was expressed at high levels in GB2–5 cells compared with U87 cells and mainly as an 18-kDa protein (Figure 1). When pleiotrophin expression was knocked down by shRNA, both sphere formation and expression levels of the stem cell markers examined were suppressed (Figures 2a and b). We found that GSCs infected with a lentivirus expressing an shRNA targeting ALK or pleiotrophin had increased levels of the neural marker mitogen-activated protein kinase 2 (*MAP2*; Supplementary Figure S1A). By contrast, knockdown of either ALK or pleiotrophin resulted in decreased expression of the astrocyte marker glial fibrillary acidic protein (*GFAP*) and the oligodendrocyte marker *Olig2* (Supplementary Figure S1A). We observed that knockdown of either ALK or pleiotrophin did not cause apoptosis (Supplementary Figure S1B) or any drastic morphological change (Supplementary Figure S1C). In addition, knockdown of pleiotrophin resulted in a decrease in ALK protein and mRNA levels, suggesting that pleiotrophin stimulates not only ALK kinase activity but also *ALK* gene expression. These results suggest that ALK and pleiotrophin are important for the self-renewal and stem-like properties of GSCs.

ALK and pleiotrophin activate the Myc and ESC-like transcriptional programs in GSCs

To study the role of the pleiotrophin-ALK axis in GSCs, we investigated the gene expression profiles of GB2 cells in which either ALK or pleiotrophin expression had been suppressed by siRNA. DNA microarray analyses revealed that the MAP kinase, phosphoinositide 3-kinase (PI3-kinase) and Janus kinase/signal transducer and activator of transcription factor (JAK/STAT) pathways are activated in GSCs (Figure 2c and Supplementary Tables S2–S4). Pleiotrophin, but not ALK, was also found to activate the Wnt signaling pathway. We found about a 30% overlap in the genes whose expression was reduced by suppression of ALK and pleiotrophin (Figure 2d and Supplementary Tables S2–S4). Furthermore, we found that downstream target genes of ALK and pleiotrophin overlap with those enriched in ESCs, which are known to be overexpressed in poorly differentiated tumors, including glioblastoma[25] (Figure 2d, upper panel and Supplementary Tables S2–S4). It had been previously reported that the NPM-ALK fusion protein induces Myc expression.[26] We also found that ALK and pleiotrophin target genes overlap those targeted by Myc and its related proteins, the Myc module, which has been reported to account for most of the similarity between ESCs and cancer cells[27] (Figure 2d, lower panel and Supplementary Tables S2–S4). These results suggest that ALK and pleiotrophin may confer a more aggressive oncogenic phenotype to glioblastomas by activating the Myc and ESC-like transcriptional programs.

ALK and pleiotrophin are critical for the tumorigenicity of GSCs

It has been suggested that the stem-like properties of GSCs are indispensable for their tumorigenicity.[3,28] We therefore attempted to clarify the involvement of the pleiotrophin-ALK axis in the tumorigenicity of GSCs. We took GB2 cells containing a

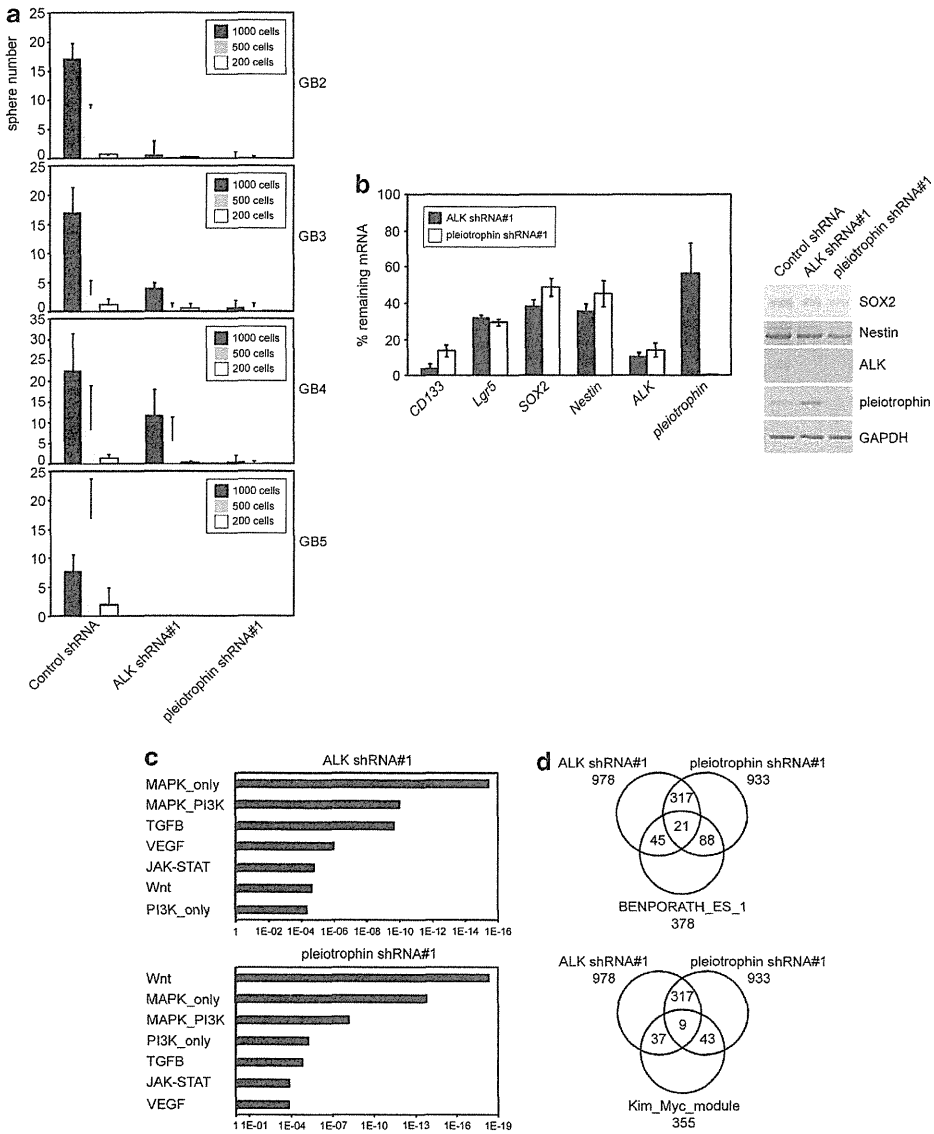

Figure 2. ALK and pleiotrophin are required for the self-renewal and stem-like properties of GSCs. (**a**) GB2–5 cells maintained in serum-free medium were infected with a lentivirus expressing an shRNA-targeting ALK or pleiotrophin. Three days after lentivirus infection, cells were trypsinized and plated at the indicated cell numbers into 96-well tissue culture plates. Two weeks after plating, the number of spheres was counted. Error bars represent the s.d. ($n = 7$–8). (**b**) GB2 cells maintained in serum-free medium were infected with a lentivirus expressing an shRNA-targeting ALK or pleiotrophin. One week after infection, the mRNA levels of the indicated genes were evaluated by quantitative RT–PCR and shown as the percentage of the remaining mRNA compared with cells expressing control shRNA (left). Error bars represent the s.d. ($n = 3$). Cell lysates were subjected to immunoblotting with antibodies to the indicated proteins (right). CD133 and Lgr5 could not be detected by immunoblotting because of their low expression levels. (**c**) GB2 cells maintained in serum-free medium were treated as described in panel (**b**). One week after infection, expression data were generated using HG-U133 plus 2.0 GeneChips. Bar graph represents signaling pathways downregulated by knockdown of ALK (upper) and pleiotrophin (lower). (**d**) Venn diagram showing the overlap among genes downregulated by knockdown of ALK (ALK_signature: ALK shRNA#1), those downregulated by knockdown of pleiotrophin (PTN_signature: pleiotrophin shRNA#1) and those enriched in ESCs (ES signature: BENPORATH_ES_1) (upper) or those targeted by Myc and its related proteins (Myc human: Kim_Myc_module) (lower). The significance of the overlap between each pair of signature is shown in Supplementary Table S4 (hypergeometric *P*-value).

lentivirus-delivered shRNA that stably suppresses ALK or pleiotrophin expression and intracranially transplanted these into immunodeficient mice. Mice receiving the ALK- or pleiotrophin-suppressed cells were found to survive longer than those transplanted with GB2 cells infected with a control lentivirus (Figure 3). Histopathological analysis of the tumor xenografts demonstrated that silencing of either ALK or pleiotrophin inhibited glioblastoma progression, whereas control GB2 cells formed invasive glioblastoma (Supplementary Figure S2). Taken together, these results suggest that the pleiotrophin-ALK axis maintains the tumorigenicity of GSCs.

High expression of pleiotrophin in GSCs

Aberrant activation of ALK by oncogenic fusion or mutation can drive tumorigenesis.[7] However, we could not identify any

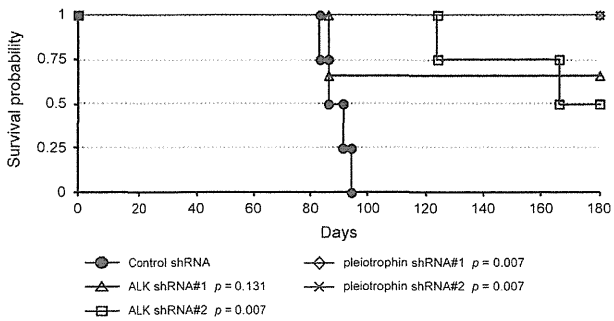

Figure 3. ALK and pleiotrophin are critical for the tumorigenicity of GSCs. GB2 cells maintained in serum-free medium were infected with a lentivirus expressing an shRNA-targeting ALK or pleiotrophin. One week after infection, cells were transplanted into the frontal lobe of immunodeficient mice. *P*-values with comparison to control shRNA by log rank test are shown.

mutation in the *ALK* gene in GB2 cells, consistent with the results of a comprehensive genome analysis reported previously.[29,30] It is known that pleiotrophin is highly expressed in GSCs (Figure 1). We therefore examined the transcriptional control of *pleiotrophin* in GSCs. We found that pleiotrophin protein and mRNA expression levels decreased during serum-induced differentiation, similar to what was observed for the stem cell markers (Figure 4a). Moreover, retinoic acid-induced differentiation also resulted in a decrease in the levels of pleiotrophin[31] (Figure 4b). We also investigated the expression profiles of *pleiotrophin* obtained from a public microarray database.[3] Almost all patient glioblastomas and two GSC lines as well as NSCs expressed substantial levels of *pleiotrophin* (Figure 4c). By contrast, glioma cell lines and two GSC lines cultured in serum-containing medium expressed relatively low levels of *pleiotrophin*, presumably because they had undergone 'differentiation'.[3] These results suggest that high expression of pleiotrophin is a common feature of GSCs.

SOX2 directly transactivates the expression of pleiotrophin in GSCs

To further investigate the mechanisms underlying the expression of *pleiotrophin*, we performed reporter assays using a *luciferase* reporter under the control of the full-length *pleiotrophin* 5′ region (−1401 to +309) and several deletion variants. When transfected into GB2 cells, a reporter containing the region between −251 and +309 showed a substantial level of activity (Figure 5a, left panel). Furthermore, this activity was repressed upon serum-induced differentiation. We therefore attempted to identify the transcription factor(s) involved in modulating this promoter activity. We first searched the region −251 and +309 for transcription factor consensus binding sites and then compared the expression patterns of the selected transcription factors and pleiotrophin using a microarray database.[3] We found that the expression pattern of *pleiotrophin* is similar to that of *SOX2* (Figure 4c). Furthermore, a mutant reporter lacking the SOX2-binding site (−40 to −21) showed reduced promoter activity (Figure 5a, right panel). Chromatin immunoprecipitation analysis demonstrated that endogenous SOX2 was present at the *pleiotrophin* promoter in GSCs (Figure 5b and Supplementary Figure S3A). Consistent with these results, silencing of SOX2 by shRNA resulted in a decrease in the levels of pleiotrophin protein and mRNA (Figure 5c and Supplementary Figure S3B). Similar results were obtained by transfecting two different siRNAs targeting SOX2 (Supplementary Figure S3C). These results suggest that SOX2 stimulates transcription of the *pleiotrophin* gene, thereby maintaining high expression levels of pleiotrophin in GSCs.

DISCUSSION

It has been reported that ALK acquires oncogenic potential when truncated and fused to a partner protein, such as NPM, as can occur via chromosomal rearrangement.[7,8] It has also been reported that ALK is activated by point mutations in its kinase domain in some neuroblastoma.[7,32] Although we could not identify any chromosomal rearrangement or point mutation in ALK in GB2 cells, we found that ALK is highly expressed in GSC lines cultured in serum-free medium, consistent with previous reports.[33] Furthermore, we showed that knockdown of ALK results in a decrease in the self-renewing capacity and tumorigenicity of GB2 cells. We also found that pleiotrophin is overexpressed both in patient glioblastomas and in GSC lines cultured in serum-free medium and that knockdown of pleiotrophin leads to a reduction in the self-renewing capacity and tumorigenicity of GB2 cells. Thus, our results suggest that the pleiotrophin-ALK axis is required for the self-renewal and tumorigenicity of GSCs.

NPM-ALK, the most thoroughly studied ALK-fusion protein, has been reported to signal via the MAP kinase, phospholipase Cγ, PI3-kinase and JAK/STAT pathways.[7] Consistent with these reports, our DNA array analysis revealed that the MAP kinase, PI3-kinase and JAK/STAT pathways are activated in GSCs. Furthermore, we found that ALK and pleiotrophin activate the Myc and ESC-like transcriptional programs, which are known to be associated with more aggressive phenotypes in human cancers.[25,27] Activation of these pathways by ALK has not been previously reported, presumably because earlier studies utilized cultured cell lines grown in serum-containing media that do not exhibit any stem cell-like properties. We found that there was only about a 30% overlap between the genes dependent on ALK and pleiotrophin expression. Furthermore, only pleiotrophin, but not ALK, activated the Wnt signaling pathway. These results appear to be in line with the fact that pleiotrophin signals not only via ALK but also via other receptors, such as RPTPβ/ζ (receptor protein tyrosine phosphatase β/ζ) and N-syndecan.[34,35] Interestingly, pleiotrophin is known to stimulate tyrosine phosphorylation of β-catenin through inactivation of RPTPβ/ζ.[34] Furthermore, pleiotrophin stimulates tumor angiogenesis and remodeling of the microenvironment.[36] Consistent with these findings, we found that repression of pleiotrophin has a more dramatic effect on the tumorigenicity of GSCs than repression of ALK.

It has been reported that SOX2 is involved in the tumorigenesis of several cancers, including lung cancer and breast cancer.[37–39] We found that SOX2 directly transactivates the expression of pleiotrophin in GSCs. Our results appear to be consistent with a previous report showing that knockdown of SOX2 suppresses the tumorigenicity of GSCs in immunodeficient mice.[17] Thus, SOX2-mediated transactivation of pleiotrophin may be important for the tumorigenicity of GSCs. However, knockdown of SOX2 only partially reduced the expression levels of pleiotrophin (Figure 5c and Supplementary Figures 3B and C), and mutation of the SOX2-binding site in the pleiotrophin promoter only partially reduced activity of a luciferase reporter (Figure 5a, right panel). In addition, we found that the levels of pleiotrophin decreased faster than those of SOX2 during serum-induced differentiation (Figure 4a) and that retinoic acid-induced differentiation resulted in a drastic decrease in the expression levels of pleiotrophin but not of SOX2 (Figure 4b). Thus, the pleiotrophin-ALK axis may be regulated by other transcription factors in addition to SOX2.

SOX2 is well known to have critical roles in the maintenance of neural stem and progenitor cells.[14,15] For example, it has been reported that multipotent neural stem-like cells transfected with an siRNA targeting SOX2 express increased neurofilaments but decreased GFAP and Nestin levels.[40] These results suggest that SOX2 inhibits the differentiation of neural stem-like cells into neurons and maintains their stem-like properties. Intriguingly, our results appear to be consistent with these results. We found that

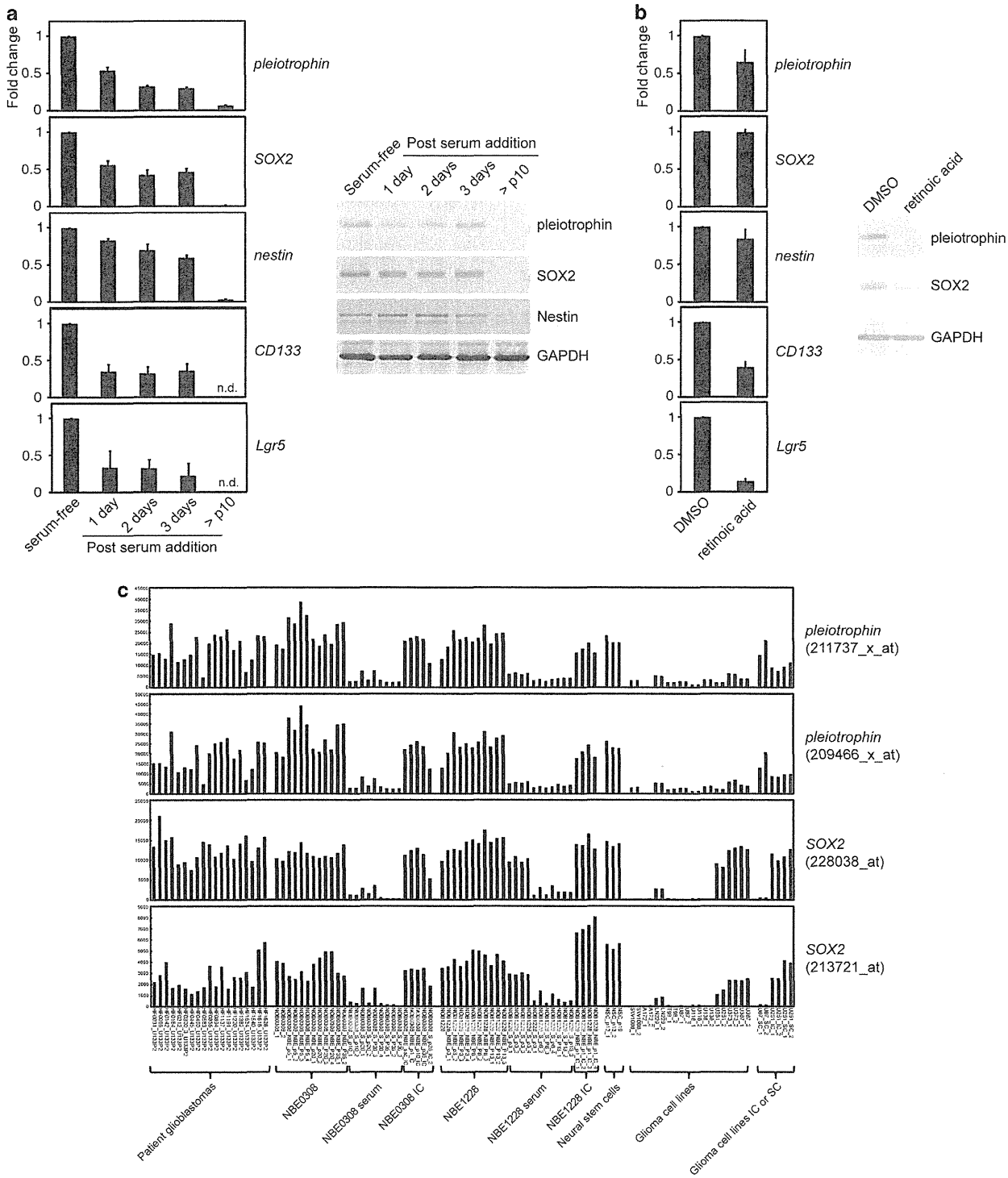

Figure 4. High expression of pleiotrophin in GSCs. (**a**) GB2 cells maintained in serum-free medium were cultured in serum-containing medium for the indicated times. >p10, GB2 cells cultured in serum-containing medium for >10 passages. The mRNA levels of the indicated genes were evaluated by quantitative RT–PCR and shown as the fold change over mRNA levels in GB2 cells maintained in serum-free medium (left). Error bars represent the s.d. ($n = 3$). ND, not detected. Cell lysates were subjected to immunoblotting with antibodies to the indicated proteins (right). CD133 and Lgr5 could not be detected by immunoblotting because of their low expression levels. (**b**) GB2 cells maintained in serum-free medium were cultured in medium containing retinoic acid for 4 days. The mRNA levels of the indicated genes were evaluated by quantitative RT–PCR and shown as the fold change over the vehicle-treated cells (left). Error bars represent the s.d. ($n = 3$). Cell lysates were subjected to immunoblotting with antibodies to the indicated proteins (right). (**c**) Gene expression profiles of *pleiotrophin* and *SOX2* taken from the public microarray database GSE4536 (Lee *et al.*[3]). Data obtained with two independent probes for each gene are shown. NBE0308 and NBE1228 are GSC lines. Serum, GSCs cultured in serum-containing medium; IC, intracranial injection; SC, subcutaneous injection.

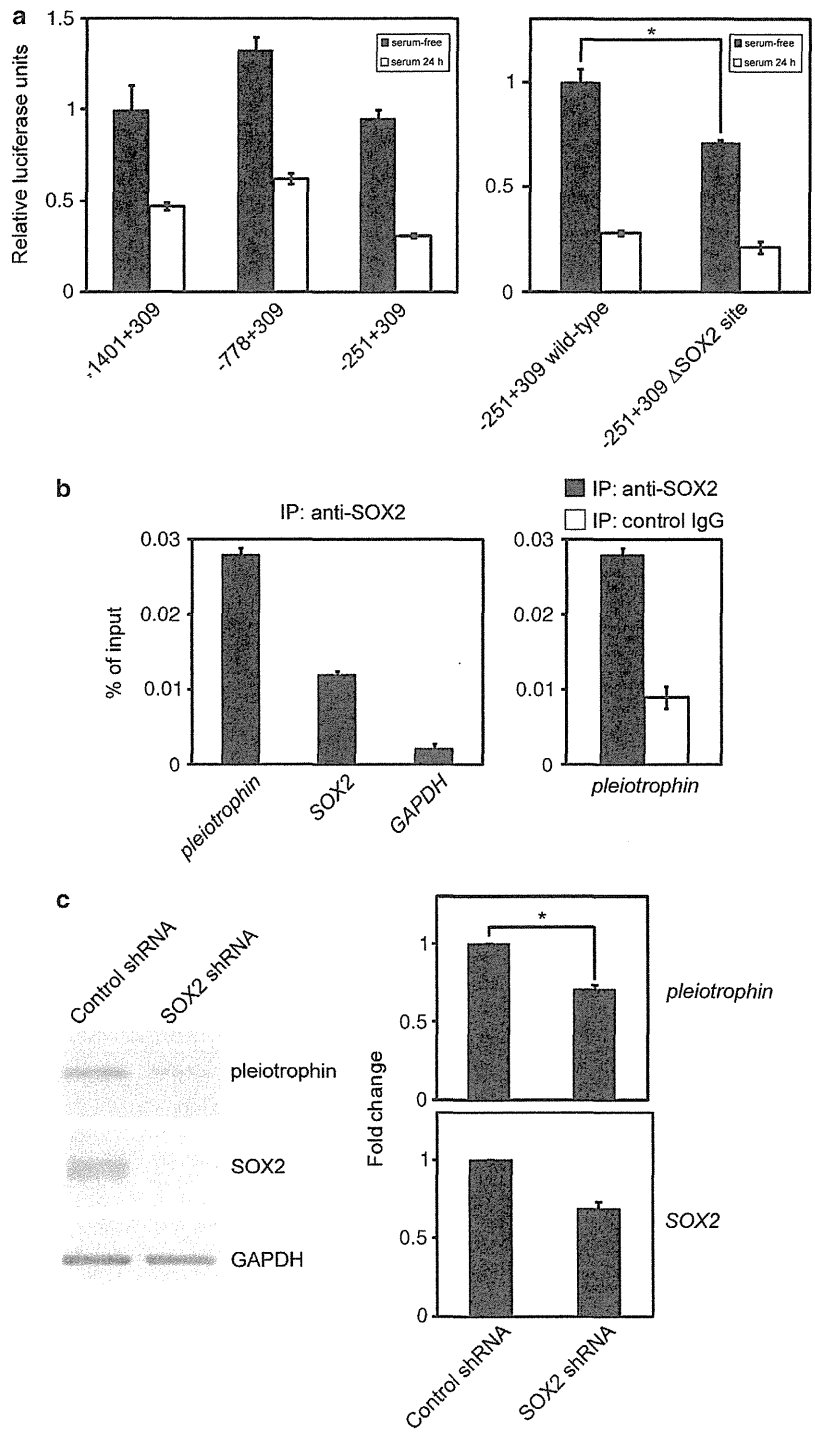

Figure 5. SOX2 directly transactivates the expression of pleiotrophin in GSCs. (**a**) GB2 cells maintained in serum-free medium were transfected with a luciferase reporter driven by the *pleiotrophin* promoter. Luciferase reporter activity is shown. Error bars represent the s.d. ($n = 3$). $^*P = 0.0058$ by *t*-test. (**b**) Chromatin immunoprecipitation experiments with anti-SOX2 antibody were performed with GB2 cells maintained in serum-free medium. The precipitated chromatin was amplified by quantitative PCR using primers flanking the indicated gene promoters (*pleiotrophin* and *GAPDH*) or enhancer (*SOX2*) (left). The *SOX2* enhancer was used as a positive control, as SOX2 has been reported to be autoregulated.[50] The *GAPDH* promoter was used as a negative control. Control IgG was used as a negative control (right). Error bars represent the s.d. ($n = 3$). (**c**) GB2 cells maintained in serum-free medium were infected with a lentivirus expressing an shRNA-targeting SOX2. Cell lysates were subjected to immunoblotting with antibodies to the indicated proteins (left). The mRNA levels of the indicated genes were evaluated by quantitative RT-PCR and shown as the fold change over mRNA levels in cells expressing control shRNA (right). Error bars represent the s.d. ($n = 3$). $^*P = 0.001$ by *t*-test.

GSCs infected with a lentivirus expressing an shRNA targeting ALK or pleiotrophin have increased MAP2 but decreased GFAP, Olig2 and Nestin levels. These results suggest that the pleiotrophin-ALK axis inhibits neural differentiation of GSCs but maintains their stem-like characteristics. It would be interesting to examine whether the pleiotrophin-ALK axis is also involved in the maintenance of normal neural stem and progenitor cells. SOX2 has also been reported to have essential roles in the neuronal differentiation of subsets of neural stem and progenitor cells.[14,15] For example, it has been reported that SOX2 deficiency causes impaired neurogenesis and neurodegeneration in the adult mouse brain.[41,42] Therefore, it would be interesting to investigate whether the pleiotrophin-ALK axis is also involved in the differentiation of neural stem and progenitor cells.

The ALK inhibitor crizotinib has recently been approved for the treatment of metastatic and late stage ALK-positive NSCLC having translocations of the ALK gene.[9,10] In addition, the ALK inhibitor TAE684 has been reported to inhibit the growth of ALK-positive ALCL, neuroblastoma and NSCLC cell lines.[43] Thus, we speculate that ALK inhibitors may be effective for the treatment of glioblastoma. ALK has been assumed to have a role in the development and function of the central and peripheral nervous system, as ALK is abundantly expressed in the nervous system during mouse embryogenesis,[7] which could raise concerns about the safety of such therapy. However, both ALK- and pleiotrophin-mutant mice survive as long as wild-type mice.[7,44] In addition, although pleiotrophin is highly expressed in NSCs, it seems dispensable for their proliferation *in vivo*.[45] Furthermore, it has been reported that the most common adverse reactions of crizotinib are relatively minor, consisting of vision disorder, nausea, diarrhea, vomiting, edema and constipation.[46] Thus, compounds targeting ALK or pleiotrophin would be expected to have relatively few serious side effects due to their effects on NSCs. In addition, we imagine that antibodies or compounds that specifically target the extracellular domain of ALK or pleiotrophin could also hold promise as novel anti-tumor reagents.

MATERIALS AND METHODS

Tumor specimens and primary tumor cultures

Tumor samples classified as primary glioblastoma were obtained from patients undergoing surgical treatment at the University of Tokyo Hospital with informed consent and as approved by the Institutional Review Board. Tumors were washed and mechanically and enzymatically dissociated into single cells. Tumor cells were cultured in Neurobasal medium (Life Technologies, Carlsbad, CA, USA) containing B27 supplement minus vitamin A (Life Technologies), EGF and FGF2 (20 ng/ml each; Wako Pure Chemical Industries, Osaka, Japan). For *in vitro* differentiation, tumor cells were cultured in DMEM (Dulbecco's modified Eagle's medium)/F-12 medium (Life Technologies) containing 10% fetal bovine serum or 10 μM all-trans retinoic acid (Sigma, St. Louis, MO, USA). U87 and 293FT cells were cultured in DMEM (Nissui, Tokyo, Japan) containing 10% fetal bovine serum. Transfections were performed using Lipofectamine 2000 Reagent, Lipofectamine LTX Reagent or Lipofectamine RNAiMAX Reagent (Life Technologies).

RNAi

Silencer Select Human Extended Druggable Genome siRNA Library was purchased from Life Technologies (the list is given in Supplementary Table S1). The siRNA oligonucleotide sequences were as follows: SOX2#1 (5′-CAGUAUUUAUCGAGAUAAA-3′), and SOX2#2 (5′-AGUG GAAACUUUUGUCGGA-3′).

The shRNA oligonucleotide sequences were as follows: ALK#1 (5′-GGCCU GUAUACCGGAUAAUGA-3′), ALK#2 (5′-GAAUACAGCACCCAAAUCAAG-3′), pleiotrophin#1 (5′-GGAGCUGAGUGCAAGCAAACC-3′), pleiotrophin#2 (5′-GCAACUGGAAGAAGCAAUUUG-3′), and SOX2 (5′-GUAAGAAACAGCAUG GAGAAA-3′).

Quantitative RT–PCR

Total RNA was extracted using the NucleoSpin RNA Clean-up kit (Takara Bio Inc., Shiga, Japan) and reverse-transcribed into cDNA using PrimeScript RT Master Mix (Takara Bio Inc.). Real-time PCR was performed using LightCycler480 SYBR Green I Master and a LightCycler480 Instrument (Roche, Indianapolis, IN, USA). The results were normalized with the detected value for glyceraldehyde-3-phosphate dehydrogenase (*GAPDH*) or hypoxanthine phosphoribosyltransferase 1 (*HPRT1*). Primers used in real-time PCR were as follows: *GAPDH* forward (5′-GCACCGTCAAGGCTGA GAAC-3′), *GAPDH* reverse (5′-TGGTGAAGACGCCAGTGGA-3′); *HPRT1* forward (5′-GGCAGTATAATCCAAAGATGGTCAA-3′), *HPRT1* reverse (5′-GTCA AGGGCATATCCTACAACAAAC-3′); *CD133* forward (5′-AGTGGCATCGTGCA AACCTG-3′), *CD133* reverse (5′-CTCCGAATCCATTCGACGATAGTA-3′); *nestin* forward (5′-GAGGTGGCCACGTACAGG-3′), *nestin* reverse (5′-AAGCTGAGGG AAGTCTTGGA-3′); *Lgr5* forward (5′-GATTTCCTGCTTGACTTTGAGG-3′), *Lgr5* reverse (5′-GCAGGTGTTCACAGGGTTTG-3′); *SOX2* forward (5′-TTGCTGCCTC TTTAAGACTAGGA-3′), *SOX2* reverse (5′-CTGGGGCTCAAACTTCTCTC-3′); *ALK* forward (5′-CACTCCAGGGAAGCATGG-3′), *ALK* reverse (5′-TCGAAATGGGTT GTCTGGA-3′); *pleiotrophin* forward (5′-AACTGACCAAGCCCAAACCT-3′), *pleiotrophin* reverse (5′-GGTGACATCTTTTAATCCAGCA-3′), *MAP2* forward (5′-TCTCCTGTGTTAAGCGGAAAA-3′), *MAP2* reverse (5′-AATACACTGGGAGC CAGAGC-3′), *GFAP* forward (5′-GACCTGGCCACTGTGAGG-3′), *GFAP* reverse (5′-AGGCAGCCAGGTTGTTCTC-3′), *Olig2* forward (5′-AGCTCCTCAAATCGC ATCC-3′), and *Olig2* reverse (5′-ATAGTCGTCGCAGCTTTCG-3′).

Antibodies

Rabbit polyclonal antibody (pAb) to green fluorescence protein (GFP) and goat pAb to SOX2 were obtained from Santa Cruz Biotechnology (Santa Cruz, CA, USA). Rabbit pAbs to ALK were from Cell Signaling Technology (Danvers, MA, USA). Mouse monoclonal antibody (mAb) to pleiotrophin (H-6) was from Santa Cruz Biotechnology. Mouse mAb to Nestin was from R&D systems (Minneapolis, MN, USA). Mouse mAb to GAPDH was from Millipore (Bedford, MA, USA).

Immunoblotting

Cells were lysed in lysis buffer (50 mM Tris-HCl (pH 7.5), 150 mM NaCl, 1% Triton X-100, 1 mM DTT, 1 mM EDTA, 2 mM Na_3VO_4, 10 mM NaF and protease inhibitors. Lysates were fractionated by SDS–PAGE (sodium dodecyl sulfate-polyacrylamide gel electrophoresis) and transferred to a PVDF (polyvinylidene difluoride) membrane (Immobilon-P, Millipore). The membrane was subjected to immunoblot analysis using alkaline phosphatase-conjugated anti-mouse immunoglobulin G (IgG) or anti-rabbit IgG (Promega, Madison, WI, USA) as secondary antibodies. Visualization was performed using the NBT/BCIP colorimetric substrate system (Promega).

Lentivirus production

A lentiviral vector (CS-Rfa-CG) expressing an shRNA driven by the H1 promoter was transfected together with the packaging vectors pCAG-HIV-gp and pCMV-VSV-G-RSV-Rev into 293FT cells. All plasmids were kindly provided by H. Miyoshi (RIKEN BioResource Center, Ibaraki, Japan). Virus supernatant was purified by ultracentrifugation at 25 000 r.p.m. for 90 min (SW28 rotor, Beckman Coulter, Brea, CA, USA). Infection efficiency was monitored by GFP expression driven by the CMV promoter.

Intracranial xenograft

One week after lentivirus infection, 1×10^4 cells were injected stereotactically into the right frontal lobe of 5-week-old nude mice (BALB/cAJcl-*nu/nu*, CLEA Japn Inc., Tokyo, Japan), following administration of general anesthesia ($n = 3$ or 4). The injection coordinates were 2 mm to the right of the midline, 1 mm anterior to the coronal suture and 3 mm deep. Mice were monitored for 6 months. Survival of mice was evaluated by Kaplan–Meier analysis. *P*-values were calculated using log rank test. The distribution of tumor cells was analyzed by GFP immunostaining. Tumors were histologically analyzed after hematoxylin and eosin staining. All animal experimental protocols were performed in accordance with the guidelines of the Animal Ethics Committee of the University of Tokyo.

Immunohistochemistry

Three months after injection of cells, brains were fixed in 3.7% buffered formalin, dehydrated and embedded in paraffin. Sections (6 μm) were rehydrated, and endogenous peroxidases were blocked by incubation in

0.3% H_2O_2 for 5 min. The primary antibody was detected using the VECTASTAIN ABC kit (Vector Laboratories, Burlingame, CA, USA). Slides were lightly counterstained with hematoxylin.

Flow cytometry

Cells were trypsinized, fixed in 70% ethanol and then stained with propidium iodide (Sigma). Cells were passed through a FACSCalibur instrument (BD Biosciences, Billerica, MA, USA).

Microarray analysis

Expression data of cells infected with a lentivirus expressing an shRNA targeting ALK or pleiotrophin were generated using HG-U133 plus 2.0 GeneChips (Affymetrix, Santa Clara, CA, USA). Normalization and analysis of the data were conducted using Gene Spring version 11.5.1 (Agilent Technologies, Santa Clara, CA, USA). Affimetrix CEL files were uploaded to GeneSpring, and RobustMulti-Array normalization was performed. Genes downregulated >1.9-fold by ALK knockdown and those downregulated >2.3-fold by pleiotrophin knockdown were termed 'ALK_signature (ALK-sig)' and 'pleiotrophin (PTN) signature (PTN-sig)' genes, respectively (the gene lists are provided in Supplementary Tables S2 and S3). BENPORATH_ES_1 were taken from the Molecular Signature Database (MSigDB).[25,47] The Kim_Myc_module was taken from Myc human module listed in Supplementary Table S3 of Kim *et al.*[27] The significance of the overlap between sh-ALK, sh-PTN#1, BENPORATH_ES_1 and/or Kim_Myc_module was calculated by the hypergeometric distribution shown in Supplementary Table S4 (Tavazoie *et al.*[48]) Functional characterization of these genes was performed using SPEED.[49] The data derived from microarray analysis has been deposited in the Gene Expression Omnibus database (GSE32482). The expression profiles of *pleiotrophin* and *SOX2* in patient glioblastomas, two GSC lines and glioma cell lines were taken from GSE4536 (Lee *et al.*[3]).

Reporter assay

Cells were transfected with a luciferase-reporter plasmid. For *in vitro* differentiation, fetal bovine serum was added to culture medium at a final concentration of 20% and cultured for an additional 24 h. Cells were lysed and firefly luciferase activity was measured with the Luciferase Reporter Assay System (Promega) and shown as the average of three measurements.

Chromatin immunoprecipitation

Cells were fixed with 1% formalin and then the reaction was stopped by the addition of glycine to a final concentration of 125 mM. Cells were lysed in chromatin immunoprecipitated lysis buffer (50 mM Tris-HCl, pH 8.0, 1% SDS, 10 mM EDTA and protease inhibitors). Lysates were sonicated to generate DNA fragments of ~1 kb in length and then diluted 10-fold to reduce the concentration of SDS to 0.1%. Immunoprecipitations were performed with an anti-SOX2 antibody. Samples were washed, reverse-crosslinked and digested by proteinase K. Purified DNA samples were analyzed by real-time PCR, and differences in the DNA content between the bound and input fractions were determined. Primers used for amplification of the gene promoters or enhancer were as follows: *pleiotrophin* forward (5′-CAGCTCTCGAGTGCAAAGC-3′), *pleiotrophin* reverse (5′-AATGGGAGGGATGAGAGGAG-3′); *GAPDH* forward (5′-TGCGTGCCCAGTT GAACCAG-3′), *GAPDH* reverse (5′-AACAGGAGGAGCAGAGAGCGAAGC-3′); *SOX2* forward (5′-TGAAGACAGTCTAGTGGGAGATGT-3′), and *SOX2* reverse (5′-CTCTTTGGCCCAGGAAACT-3′).

CONFLICT OF INTEREST

The authors declare no conflict of interest.

ACKNOWLEDGEMENTS

This work was supported by the Research Program of Innovative Cell Biology by Innovative Technology (Integrated Systems Analysis of Cellular Oncogenic Signaling Networks), Grants-in-Aid for Scientific Research on Innovative Areas (Integrative Research on Cancer Microenvironment Network), Takeda Science Foundation and, in part, by Global COE Program (Integrative Life Science Based on the Study of Biosignaling Mechanisms), MEXT, Japan.

REFERENCES

1 Furnari FB, Fenton T, Bachoo RM, Mukasa A, Stommel JM, Stegh A *et al.* Malignant astrocytic glioma: genetics, biology, and paths to treatment. *Genes Dev* 2007; **21**: 2683–2710.
2 Chen J, McKay RM, Parada LF. Malignant glioma: lessons from genomics, mouse models, and stem cells. *Cell* 2012; **149**: 36–47.
3 Lee J, Kotliarova S, Kotliarov Y, Li A, Su Q, Donin NM *et al.* Tumor stem cells derived from glioblastomas cultured in bFGF and EGF more closely mirror the phenotype and genotype of primary tumors than do serum-cultured cell lines. *Cancer Cell* 2006; **9**: 391–403.
4 Sell S. Cancer stem cells and differentiation therapy. *Tumour Biol* 2006; **27**: 59–70.
5 Zhang J, Yang PL, Gray NS. Targeting cancer with small molecule kinase inhibitors. *Nat Rev Cancer* 2009; **9**: 28–39.
6 Kadomatsu K, Muramatsu T. Midkine and pleiotrophin in neural development and cancer. *Cancer Lett* 2004; **204**: 127–143.
7 Palmer RH, Vernersson E, Grabbe C, Hallberg B. Anaplastic lymphoma kinase: signalling in development and disease. *Biochem J* 2009; **420**: 345–361.
8 Turner SD, Alexander DR. What have we learnt from mouse models of NPM-ALK-induced lymphomagenesis? *Leukemia* 2005; **19**: 1128–1134.
9 Camidge DR, Doebele RC. Treating ALK-positive lung cancer--early successes and future challenges. *Nat Rev Clin Oncol* 2012; **9**: 268–277.
10 Gandhi L, Janne PA. Crizotinib for ALK-rearranged non-small cell lung cancer: a new targeted therapy for a new target. *Clin Cancer Res* 2012; **18**: 3737–3742.
11 Stylianou DC, Auf der Maur A, Kodack DP, Henke RT, Hohn S, Toretsky JA *et al.* Effect of single-chain antibody targeting of the ligand-binding domain in the anaplastic lymphoma kinase receptor. *Oncogene* 2009; **28**: 3296–3306.
12 Yuan H, Corbi N, Basilico C, Dailey L. Developmental-specific activity of the FGF-4 enhancer requires the synergistic action of Sox2 and Oct-3. *Genes Dev* 1995; **9**: 2635–2645.
13 Avilion AA, Nicolis SK, Pevny LH, Perez L, Vivian N, Lovell-Badge R. Multipotent cell lineages in early mouse development depend on SOX2 function. *Genes Dev* 2003; **17**: 126–140.
14 Sarkar A, Hochedlinger K. The Sox family of transcription factors: versatile regulators of stem and progenitor cell fate. *Cell Stem Cell* 2013; **12**: 15–30.
15 Episkopou V. SOX2 functions in adult neural stem cells. *Trends Neurosci* 2005; **28**: 219–221.
16 Schmitz M, Temme A, Senner V, Ebner R, Schwind S, Stevanovic S *et al.* Identification of SOX2 as a novel glioma-associated antigen and potential target for T cell-based immunotherapy. *Br J Cancer* 2007; **96**: 1293–1301.
17 Gangemi RM, Griffero F, Marubbi D, Perera M, Capra MC, Malatesta P *et al.* SOX2 silencing in glioblastoma tumor-initiating cells causes stop of proliferation and loss of tumorigenicity. *Stem Cells* 2009; **27**: 40–48.
18 Lottaz C, Beier D, Meyer K, Kumar P, Hermann A, Schwarz J *et al.* Transcriptional profiles of CD133+ and CD133- glioblastoma-derived cancer stem cell lines suggest different cells of origin. *Cancer Res* 2010; **70**: 2030–2040.
19 Koyama-Nasu R, Nasu-Nishimura Y, Todo T, Ino Y, Saito N, Aburatani H *et al.* The critical role of cyclin D2 in cell cycle progression and tumorigenicity of glioblastoma stem cells. *Oncogene* (e-pub ahead of print 10 September 2012; doi:10.1038/onc.2012.399).
20 Mizrak D, Brittan M, Alison M. CD133: molecule of the moment. *J Pathol* 2008; **214**: 3–9.
21 Barker N, van Es JH, Kuipers J, Kujala P, van den Born M, Cozijnsen M *et al.* Identification of stem cells in small intestine and colon by marker gene Lgr5. *Nature* 2007; **449**: 1003–1007.
22 Wurdak H, Zhu S, Romero A, Lorger M, Watson J, Chiang CY *et al.* An RNAi screen identifies TRRAP as a regulator of brain tumor-initiating cell differentiation. *Cell Stem Cell* 2010; **6**: 37–47.
23 Powers C, Aigner A, Stoica GE, McDonnell K, Wellstein A. Pleiotrophin signaling through anaplastic lymphoma kinase is rate-limiting for glioblastoma growth. *J Biol Chem* 2002; **277**: 14153–14158.
24 Galli R, Binda E, Orfanelli U, Cipelletti B, Gritti A, De Vitis S *et al.* Isolation and characterization of tumorigenic, stem-like neural precursors from human glioblastoma. *Cancer Res* 2004; **64**: 7011–7021.
25 Ben-Porath I, Thomson MW, Carey VJ, Ge R, Bell GW, Regev A *et al.* An embryonic stem cell-like gene expression signature in poorly differentiated aggressive human tumors. *Nat Genet* 2008; **40**: 499–507.
26 Raetz EA, Perkins SL, Carlson MA, Schooler KP, Carroll WL, Virshup DM. The nucleophosmin-anaplastic lymphoma kinase fusion protein induces c-Myc expression in pediatric anaplastic large cell lymphomas. *Am J Pathol* 2002; **161**: 875–883.
27 Kim J, Woo AJ, Chu J, Snow JW, Fujiwara Y, Kim CG *et al.* A Myc network accounts for similarities between embryonic stem and cancer cell transcription programs. *Cell* 2010; **143**: 313–324.
28 Singh SK, Hawkins C, Clarke ID, Squire JA, Bayani J, Hide T *et al.* Identification of human brain tumour initiating cells. *Nature* 2004; **432**: 396–401.

29 Parsons DW, Jones S, Zhang X, Lin JC, Leary RJ, Angenendt P *et al.* An integrated genomic analysis of human glioblastoma multiforme. *Science* 2008; **321**: 1807–1812.
30 Cancer Genome Atlas Research Network. Comprehensive genomic characterization defines human glioblastoma genes and core pathways. *Nature* 2008; **455**: 1061–1068.
31 Ying M, Wang S, Sang Y, Sun P, Lal B, Goodwin CR *et al.* Regulation of glioblastoma stem cells by retinoic acid: role for Notch pathway inhibition. *Oncogene* 2011; **30**: 3454–3467.
32 Carpenter EL, Mosse YP, Targeting ALK. in neuroblastoma--preclinical and clinical advancements. *Nat Rev Clin Oncol* 2012; **9**: 391–399.
33 Dirks WG, Fahrnich S, Lis Y, Becker E, MacLeod RA, Drexler HG. Expression and functional analysis of the anaplastic lymphoma kinase (ALK) gene in tumor cell lines. *Int J Cancer* 2002; **100**: 49–56.
34 Meng K, Rodriguez-Pena A, Dimitrov T, Chen W, Yamin M, Noda M *et al.* Pleiotrophin signals increased tyrosine phosphorylation of β-catenin through inactivation of the intrinsic catalytic activity of the receptor-type protein tyrosine phosphatase beta/zeta. *Proc Natl Acad Sci USA* 2000; **97**: 2603–2608.
35 Raulo E, Chernousov MA, Carey DJ, Nolo R, Rauvala H. Isolation of a neuronal cell surface receptor of heparin binding growth-associated molecule (HB-GAM). Identification as N-syndecan (syndecan-3). *J Biol Chem* 1994; **269**: 12999–13004.
36 Perez-Pinera P, Chang Y, Deuel TF. Pleiotrophin, a multifunctional tumor promoter through induction of tumor angiogenesis, remodeling of the tumor microenvironment, and activation of stromal fibroblasts. *Cell Cycle* 2007; **6**: 2877–2883.
37 Bernhardt M, Galach M, Novak D, Utikal J. Mediators of induced pluripotency and their role in cancer cells—current scientific knowledge and future perspectives. *Biotechnol J* 2012; **7**: 810–821.
38 Chen S, Xu Y, Chen Y, Li X, Mou W, Wang L *et al.* SOX2 gene regulates the transcriptional network of oncogenes and affects tumorigenesis of human lung cancer cells. *PLoS One* 2012; **7**: e36326.
39 Leis O, Eguiara A, Lopez-Arribillaga E, Alberdi MJ, Hernandez-Garcia S, Elorriaga K *et al.* Sox2 expression in breast tumours and activation in breast cancer stem cells. *Oncogene* 2012; **31**: 1354–1365.
40 Kondo T, Raff M. Chromatin remodeling and histone modification in the conversion of oligodendrocyte precursors to neural stem cells. *Genes Dev* 2004; **18**: 2963–2972.
41 Ferri AL, Cavallaro M, Braid D, Di Cristofano A, Canta A, Vezzani A *et al.* Sox2 deficiency causes neurodegeneration and impaired neurogenesis in the adult mouse brain. *Development* 2004; **131**: 3805–3819.
42 Cavallaro M, Mariani J, Lancini C, Latorre E, Caccia R, Gull F *et al.* Impaired generation of mature neurons by neural stem cells from hypomorphic Sox2 mutants. *Development* 2008; **135**: 541–557.
43 McDermott U, Iafrate AJ, Gray NS, Shioda T, Classon M, Maheswaran S *et al.* Genomic alterations of anaplastic lymphoma kinase may sensitize tumors to anaplastic lymphoma kinase inhibitors. *Cancer Res* 2008; **68**: 3389–3395.
44 Amet LE, Lauri SE, Hienola A, Croll SD, Lu Y, Levorse JM *et al.* Enhanced hippocampal long-term potentiation in mice lacking heparin-binding growth-associated molecule. *Mol Cell Neurosci* 2001; **17**: 1014–1024.
45 Hienola A, Pekkanen M, Raulo E, Vanttola P, Rauvala H. HB-GAM inhibits proliferation and enhances differentiation of neural stem cells. *Mol Cell Neurosci* 2004; **26**: 75–88.
46 Melosky B. Supportive care treatments for toxicities of anti-egfr and other targeted agents. *Curr Oncol* 2012; **19**: S59–S63.
47 Subramanian A, Tamayo P, Mootha VK, Mukherjee S, Ebert BL, Gillette MA *et al.* Gene set enrichment analysis: a knowledge-based approach for interpreting genome-wide expression profiles. *Proc Natl Acad Sci USA* 2005; **102**: 15545–15550.
48 Tavazoie S, Hughes JD, Campbell MJ, Cho RJ, Church GM. Systematic determination of genetic network architecture. *Nat Genet* 1999; **22**: 281–285.
49 Parikh JR, Klinger B, Xia Y, Marto JA, Bluthgen N. Discovering causal signaling pathways through gene-expression patterns. *Nucleic Acids Res* 2010; **38**: W109–W117.
50 Chew JL, Loh YH, Zhang W, Chen X, Tam WL, Yeap LS *et al.* Reciprocal transcriptional regulation of Pou5f1 and Sox2 via the Oct4/Sox2 complex in embryonic stem cells. *Mol Cell Biol* 2005; **25**: 6031–6046.

Supplementary Information accompanies this paper on the Oncogene website (http://www.nature.com/onc)

Oncogene (2013) **32,** 3840–3845

www.nature.com/onc

ORIGINAL ARTICLE

The critical role of cyclin D2 in cell cycle progression and tumorigenicity of glioblastoma stem cells

R Koyama-Nasu[1,4], Y Nasu-Nishimura[1,4], T Todo[2], Y Ino[2], N Saito[2], H Aburatani[3], K Funato[1], K Echizen[1], H Sugano[1], R Haruta[1], M Matsui[1], R Takahashi[1], E Manabe[1], T Oda[1] and T Akiyama[1]

Cancer stem cells are believed to be responsible for tumor initiation and development. Much current research on human brain tumors is focused on the stem-like properties of glioblastoma stem cells (GSCs). However, little is known about the molecular mechanisms of cell cycle regulation that discriminate between GSCs and differentiated glioblastoma cells. Here we show that cyclin D2 is the cyclin that is predominantly expressed in GSCs and suppression of its expression by RNA interference causes G1 arrest *in vitro* and growth retardation of GSCs xenografted into immunocompromised mice *in vivo*. We also demonstrate that the expression of *cyclin D2* is suppressed upon serum-induced differentiation similar to what was observed for the cancer stem cell marker *CD133*. Taken together, our results demonstrate that cyclin D2 has a critical role in cell cycle progression and the tumorigenicity of GSCs.

Oncogene (2013) **32,** 3840–3845; doi:10.1038/onc.2012.399; published online 10 September 2012

Keywords: cancer stem cells; cell cycle; cyclin D2; glioblastoma

INTRODUCTION

Glioblastoma is the most common primary brain tumor in adults.[1] Patients diagnosed with glioblastoma have a median survival of <1 year with generally poor responses to all therapeutic modalities. The existence of cancer stem cells responsible for tumor initiation and development has been demonstrated in a variety of tumors.[2] The discovery of glioblastoma stem cells (GSCs) was made by applying techniques for cell culture and analysis of normal neural stem cells (NSCs) to brain tumor cell populations.[3] Glioblastoma cells cultured in serum-free media supplemented with epidermal growth factor and basic fibroblast growth factor form spheres and maintain stem cell-like properties and tumorigenicity, but when grown under serum-containing culture conditions, glioblastoma cells undergo irreversible differentiation and lose their tumorigenicity.[4] Therefore, the mechanisms of maintaining the stem-like properties of GSCs have been studied extensively.

D-type cyclins are known to have critical roles in cell cycle progression.[5] Three D-type cyclins, cyclin D1, D2 and D3, are encoded by distinct genes, but show significant amino-acid similarity. Among these, cyclin D1 was first discovered and has been studied most extensively. D-type cyclins associate with partner cyclin-dependent kinases, CDK4 and CDK6, and promote phosphorylation and subsequent inactivation of the retinoblastoma tumor suppressor gene product, RB and RB-related proteins. This causes the release or de-repression of the E2F transcription factors and allows cells to enter the S phase. Dysregulation of the G1/S transition appears to be a common event in tumorigenesis.[6] Indeed, alterations in important components of the RB pathway are frequently observed in a variety of tumors, including glioblastoma.[6–8] In this study, we investigate the role of cyclin D2 in cell cycle progression and the tumorigenicity of GSCs.

RESULTS

Predominant expression of cyclin D2 in GSCs

We cultured GSCs isolated from four patients, GB1–3 and 5, under serum-free conditions that favor NSC growth.[4] Our DNA array analysis revealed that GB1 and GB2, 3 and 5 belong to the mesenchymal and proneural groups, respectively[9] (Supplementary Figure 1A). *In vitro* differentiation was induced in medium containing fetal bovine serum.[4] Differentiated GB1–3 cells proliferated more rapidly than their parental undifferentiated cells did (data not shown). By contrast, proliferation of GB5 cells was inhibited in medium containing serum (Supplementary Figure 2). Consistent with these properties, immunoblotting analysis using anti-RB antibodies revealed that RB was highly phosphorylated in differentiated GB1–3 cells and undifferentiated GB5 cells (Figure 1a). These differences may reflect the properties associated with the primary tumors from which they were derived.

To study the molecular mechanisms of cell cycle regulation in GSCs, lysates from glioblastoma cells were subjected to immunoblotting analysis with antibodies to various cyclins. We found that cyclin D2 was abundantly expressed in undifferentiated GB2, 3 and 5 cells, but was barely expressed in differentiated GB2, 3 and 5 cells, which had been cultured in serum-containing medium (Figure 1a). By contrast, cyclin D1 expression was higher in differentiated than in undifferentiated glioblastoma cells. The expression levels of cyclin D3 did not change significantly. In GB1 cells, cyclin D2 expression was not detected in either

[1]Laboratory of Molecular and Genetic Information, Institute of Molecular and Cellular Biosciences, The University of Tokyo, Bunkyo-ku, Tokyo, Japan; [2]Department of Neurosurgery, The University of Tokyo Hospital, Bunkyo-ku, Tokyo, Japan and [3]Genome Science Division, Research Center for Advanced Science and Technology, The University of Tokyo, Meguro-ku, Tokyo, Japan. Correspondence: Professor T Akiyama, Laboratory of Molecular and Genetic Information, Institute of Molecular and Cellular Biosciences, The University of Tokyo, 1-1-1, Yayoi, Bunkyo-ku, Tokyo 110-0032, Japan.
Email: akiyama@iam.u-tokyo.ac.jp
[4]These authors contributed equally to this work.
Received 22 February 2012; revised 29 June 2012; accepted 20 July 2012; published online 10 September 2012

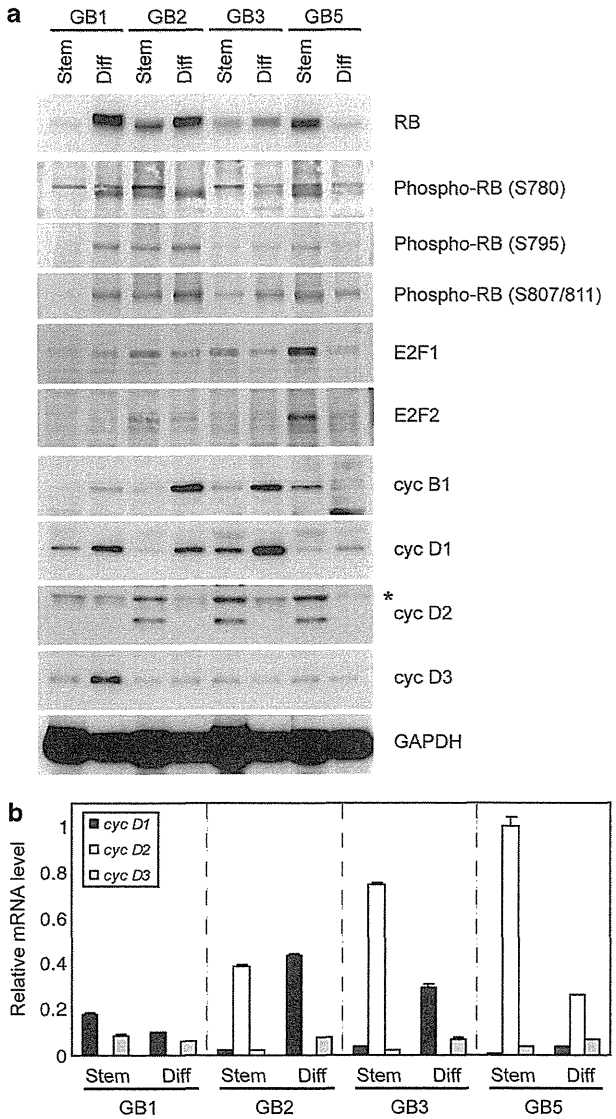

Figure 1. Predominant expression of cyclin D2 in GSCs. (**a**) Lysates from undifferentiated (stem) or differentiated (diff) GB1–3 and 5 cells were immunoblotted with antibodies to the indicated proteins. The asterisk indicates a non-specific band. (**b**) The mRNA levels of D-type cyclins in undifferentiated (stem) or differentiated (diff) GB1–3 and 5 cells were evaluated by quantitative RT–PCR. Error bars represent the s.d. ($n = 3$).

the undifferentiated or differentiated state. This may be a common feature in the mesenchymal subtype of glioblastoma (Supplementary Figure 1B). Reverse transcription–polymerase chain reaction (RT–PCR) analysis also revealed that *cyclin D2* messenger RNA (mRNA) was predominantly expressed in undifferentiated GB2, 3 and 5 cells (Figure 1b).

GSC-specific expression of cyclin D2

To further investigate the expression pattern of cyclin D2, we focused our analyses on GB2, as cyclin D2 is highly expressed and its expression is dramatically reduced by serum-induced differentiation in these cells. Time-course experiments showed that following serum addition, undifferentiated GB2 cells became attached to the bottom of the dish and formed a monolayer (Supplementary Figure 3A), as reported previously.[4] The expression levels of *cyclin D2* was significantly decreased within one day after serum addition and was completely downregulated in late-passage cells (>10 passages), similar to what was observed for the cancer stem cell marker *CD133* (Mizrak *et al.*[10]) and the NSC marker *nestin*[11] (Figure 2a, left panel). By contrast, *cyclin D1* mRNA was induced upon serum stimulation and highly expressed in late-passage cells. However, when differentiated GB2 cells (>10 passages) were cultured in serum-free conditions, cells started to form nonadherent, multicellular spheres indistinguishable from undifferentiated GSCs (Supplementary Figure 3B). Nevertheless, the expression levels of *cyclin D2* as well as *CD133* and *nestin* were not fully restored by serum deprivation (Figure 2a, right panel).

We also investigated the expression profiles of D-type cyclins in patient glioblastomas, commonly used glioma cell lines and normal human NSCs taken from a public microarray database (Figure 2b). As expected, almost all patient glioblastomas expressed substantial levels of *cyclin D2*, whereas no glioma cell line did. *Cyclin D1* was highly expressed in the glioma cell lines. Moreover, the expression of *cyclin D2* as well as *CD133* and *nestin* was not restored by serum withdrawal in the glioma cell line T98G, U251 or U87 (Figure 2c). Furthermore, either overexpression of p21 or depletion of E2F1 and/or E2F2 did not lead to the restoration of *cyclin D2* expression (Supplementary Figures 4A–D). These data are compatible with the notion that these cell lines have become differentiated under serum-containing conditions. Interestingly, *cyclin D2* and *D3*, but not *cyclin D1*, were found to be expressed in human NSCs. *Cyclin D3* and *D1* showed a reciprocal expression pattern in the glioma cell lines.

We next investigated the expression profiles of D-type cyclins in various histological grades of gliomas. The expression levels of *cyclin D2*, but not of *cyclin D1* or *D3*, were found to be significantly upregulated in glioblastomas (grade IV) compared with astrocytomas (grade II or III) and non-tumor tissues (Supplementary Figure 5 and Supplementary Table 1). Taken together, these data raise the possibility that cyclin D2 expression may be a common feature of GSCs.

Important role of cyclin D2 in cell cycle progression of GSCs

We next examined the role of cyclin D2 in cell cycle progression of GSCs using small interference RNA (siRNA). Flow-cytometric analyses of DNA content in undifferentiated GB2 cells showed that knockdown of cyclin D2, but not of cyclin D1 and/or D3, resulted in a significant increase in the fraction of cells in the G1 phase (Figure 3a, left panel). Consistent with this result, knockdown of cyclin D2 led to an increase in the amount of the hypophosphorylated form of RB, suggesting that the activity of CDK4 and/or CDK6 was suppressed and cells were arrested in the G1 phase of the cell cycle (Figure 3b, left panel). Silencing of cyclin D2 expression also caused a reduction in the level of cyclin B1, the expression of which is known to be low in the G1 phase (Figure 3b, left panel). In addition, knockdown of cyclin D2 resulted in a slight decrease in the expression levels of E2F1 and E2F2. We also observed that ectopic expression of cyclin D1 or D3 partially rescued the reduction in RB expression and phosphorylation caused by knockdown of cyclin D2. Thus, a certain amount of D-type cyclins may be required for cell cycle progression of undifferentiated GB2 cells (Supplementary Figure 6). By contrast, knockdown of cyclin D1, but not of cyclin D2 or D3, induced G1 arrest of differentiated GB2 cells cultured in serum-containing medium (Figures 3a and b, right panels). In addition, although amplification of the *cdk4* locus has been detected at a higher frequency than that of the *cdk6* locus,[7] we found that both CDK4 and CDK6 are responsible for phosphorylation of RB in undifferentiated GB2 cells (Supplementary Figures 7A and B). These results suggest that the cyclin D2–CDK4/6 complexes have an important role in cell cycle progression of undifferentiated, but not of differentiated, GSCs.

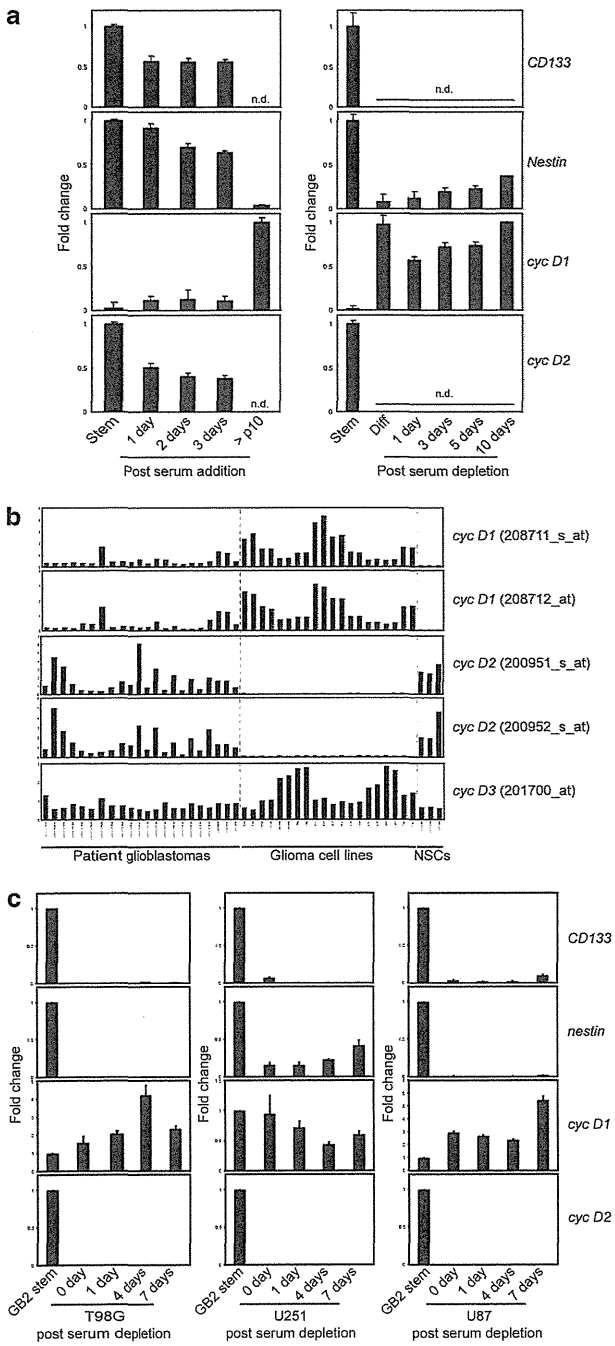

Figure 2. GSC-specific expression of *cyclin D2*. (**a**) Undifferentiated (stem) GB2 cells were cultured in medium containing serum for the indicated times (left). Differentiated (diff) GB2 cells were cultured in serum-free medium for the indicated times (right). The mRNA levels of the indicated genes were evaluated by quantitative RT–PCR and shown as fold change over mRNA levels in GB2 stem cells. Error bars represent the s.d. ($n=3$). ND means not detected. (**b**) Gene expression profiles of D-type cyclins taken from a public microarray database (GSE4536) (Lee *et al.*[4]). Data of two independent probes for *cyclin D1* and *D2*, and one probe for *cyclin D3* are shown. (**c**) The glioma cell lines T98G, U251 and U87 were cultured in serum-free medium for the indicated times. The mRNA levels of the indicated genes were evaluated by quantitative RT–PCR and shown as fold change over mRNA levels in GB2 stem cells.

Critical role of cyclin D2 in the tumorigenicity of GSCs

To clarify the significance of cyclin D2 expression in the tumorigenicity of GSCs, we transplanted GB2 cells into the frontal lobe of immunocompromised mice. As reported previously,[4] all mice transplanted with undifferentiated GB2 cells developed tumors and died within 2 months, whereas mice transplanted with differentiated GB2 cells survived over 5 months (Figure 4a). Histopathological analyses of tumor xenografts demonstrated that undifferentiated GB2 cells formed a highly invasive tumor spreading across the hemispheres, which represents an important feature of human glioblastoma (Figure 4b). RT–PCR analysis using human-specific primers demonstrated that the xenograft tumor still maintained the predominant expression of *cyclin D2* (Figure 4c and Supplementary Figure 8A). Consistent with this observation, when mice were transplanted with undifferentiated GB2 cells in which cyclin D2 expression was stably repressed by lentivirus-delivered short hairpin RNAs (shRNAs) (Supplementary Figures 8B and C), they survived significantly longer than those transplanted with undifferentiated GB2 cells infected with control lentivirus (Figure 4a). By contrast, overexpression of cyclin D2 did not restore *CD133* and *nestin* expression, as well as tumorigenicity of differentiated GB2 cells (Supplementary Figures 9A-C). These results suggest that cyclin D2 has a critical role in the tumorigenicity of GSCs.

DISCUSSION

A number of molecular studies have identified critical genetic events in glioblastoma, including the following: dysregulation of growth factor signaling; activation of the phosphatidylinositol-3-OH kinase pathway; and inactivation of the p53 and RB pathways.[7,8] Among those three core pathways, the RB pathway is obviously the most important for the regulation of G1/S progression.[6] Actually, 78% of glioblastomas are shown to harbor RB pathway aberrations, such as deletion of the *cdkn2a/cdkn2b* locus, amplification of the *cdk4* locus and deletion or inactivating mutations in *RB1* (Cancer Genome Atlas Research Network[7]). Importantly, amplification of the *cyclin D2* locus is also reported.[7] In this study, we have shown that cyclin D2 is the most abundantly expressed cyclin in GSCs among the three D-type cyclins. Moreover, suppression of cyclin D2 expression by RNA interference caused G1 arrest *in vitro* and growth retardation of GSCs xenografted into immunocompromised mice *in vivo*. Altogether, these data suggest the critical role of cyclin D2 in cell cycle progression and the tumorigenicity of GSCs.

Tumor cells in culture are valuable for studying the mechanisms of tumorigenesis. Growth media containing serum have been used for maintaining a variety of cancer cells, including glioblastoma. However, it has been shown that serum causes irreversible differentiation of GSCs.[4] Differentiated GSCs have gene expression profiles that are different from those of their parental GSCs and NSCs, and are neither clonogenic nor tumorigenic.[4] Our study shows that cyclin D2 expression is silenced when GSCs are cultured in the presence of serum. We also found that cyclin D1 expression is enhanced during serum-induced differentiation of GSCs. These results explain why commonly used glioblastoma cell lines abundantly express cyclin D1, but not cyclin D2.

It has been shown that GSCs and NSCs share similar properties such as the potential for self-renewal and differentiation.[12] Intriguingly, cyclin D2 has been reported to be the only D-type cyclin expressed in adult mouse NSCs.[13,14] Thus, it is interesting to speculate that the predominant expression of cyclin D2 in GSCs may be the reflection of the property associated with adult NSCs. It is possible that transcription factors that are important for the maintenance of the stem cell state may also be involved in cyclin D2 expression. It may also be possible that DNA

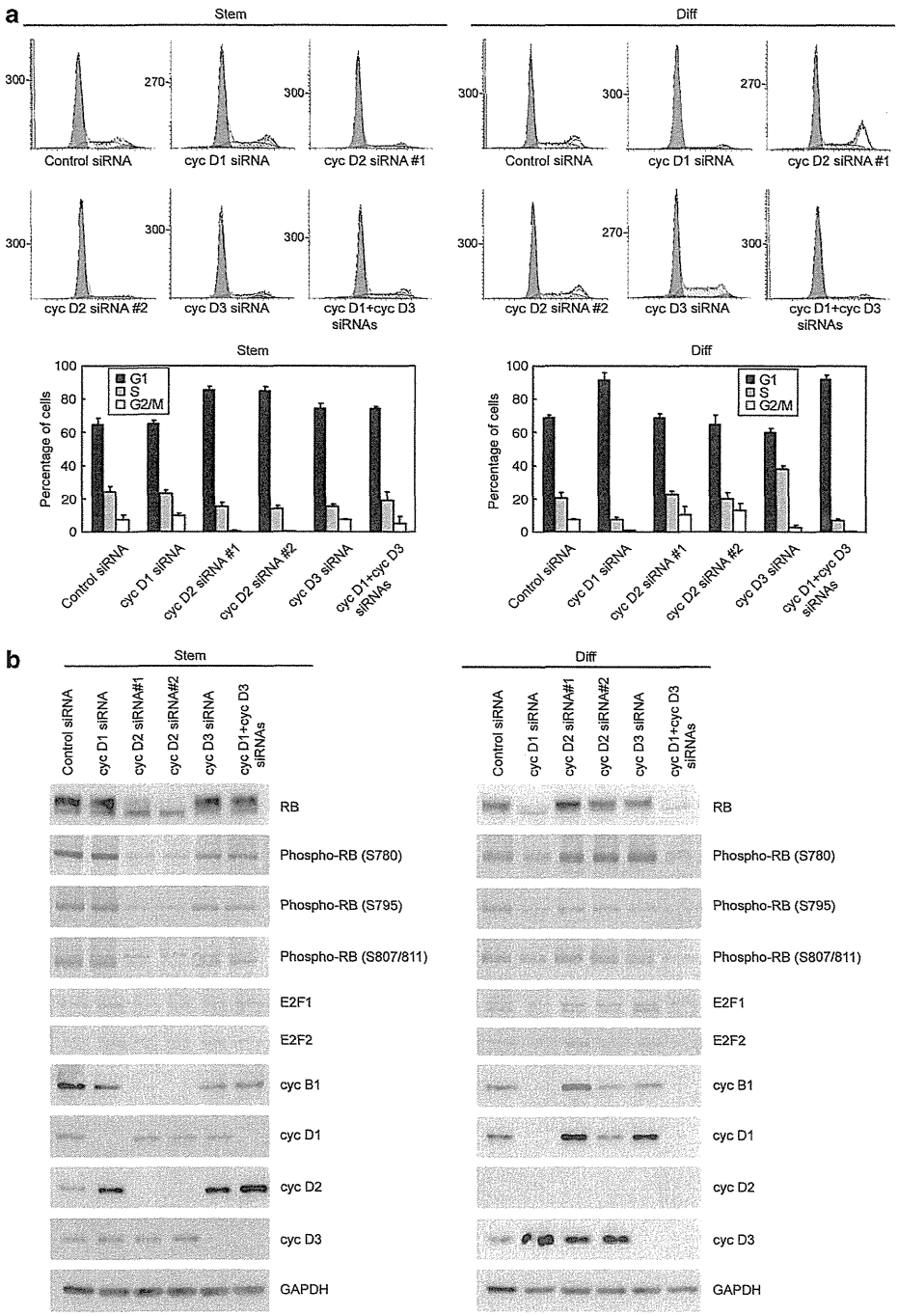

Figure 3. Important role of cyclin D2 in cell cycle progression of GSCs. (**a**) Undifferentiated (stem) (left) or differentiated (diff) (right) GB2 cells were transfected with siRNAs targeting D-type cyclins. After 72 h, cells were fixed, stained with propidium iodide and analyzed by flow cytometry for DNA content. The *x* axis represents DNA content and the *y* axis the number of cells (upper). The bar graph represents the percentages of cells in G1, S and G2/M (lower). Error bars represent the s.d. ($n = 3$). (**b**) Undifferentiated (stem) (left) or differentiated (diff) (right) GB2 cells were transfected with siRNAs targeting D-type cyclins. After 72 h, lysates were immunoblotted with antibodies to the indicated proteins.

methylation and/or mRNA stabilization by alternative cleavage- and polyadenylation-mediated shortening of 3′-UTR are involved in the alteration in cyclin D2 expression.[15]

It is important to define reliable markers that are expressed in cancer stem cells. Overexpression of cyclin D1 has been implicated in the pathogenesis of various human cancers.[5,6,16] However, our results raise the possibility that cyclin D2, rather than cyclin D1, could be a novel prognostic marker for glioblastoma. Hence, it is intriguing to perform univariate and multivariate analyses to compare the expression levels of cyclin D2 with tumorigenic capacity and tumor invasiveness.

As cancer stem cells are considered to be responsible for tumor initiation and development, GSCs may be promising targets for the therapy of glioblastoma. We therefore speculate that inhibitors

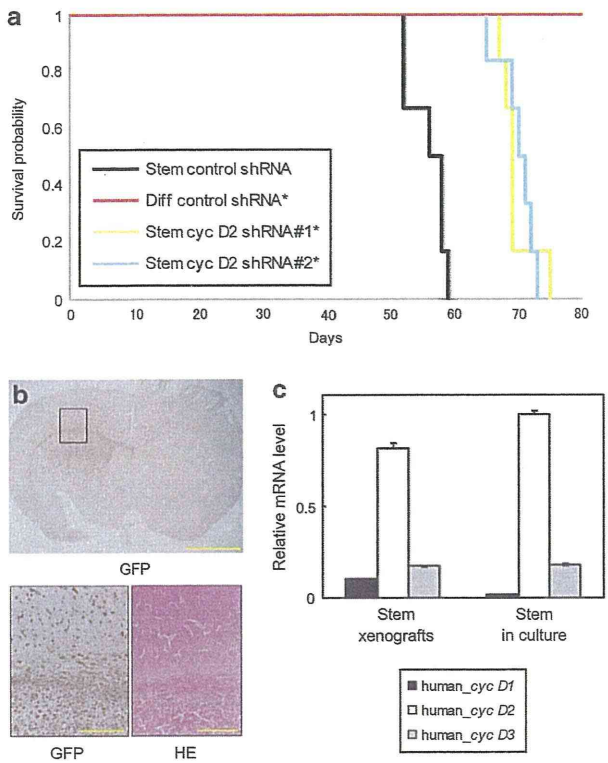

Figure 4. Critical role of cyclin D2 in the tumorigenicity of GSCs. (**a**) Undifferentiated (stem) or differentiated (diff) GB2 cells were infected with lentivirus harboring an shRNA targeting cyclin D2. After 1 week, cells were transplanted into the frontal lobe of immunocompromised mice. $*P = 0.0006$ with comparison to stem control shRNA. (**b**) Histopathological analysis of representative tumor xenograft. Undifferentiated GB2 cells were infected with control lentivirus expressing GFP and transplanted into immunocompromised mice. GFP immunostaining (distribution of tumor cells) and hematoxylin and eosin (HE) staining are shown. Scale bars represent 2 mm (upper) and 200 μm (lower). (**c**) The mRNA levels of D-type cyclins in undifferentiated (stem) GB2 xenografts and undifferentiated (stem) GB2 cells in culture were evaluated by quantitative RT–PCR using human-specific primers. Error bars represent the s.d. ($n = 3$).

that block the expression of cyclin D2 could have a growth inhibitory effect on GSCs.

MATERIALS AND METHODS

Tumor specimens and primary tumor cultures

Following informed consent, tumor samples classified as primary glioblastoma were obtained from patients undergoing surgical treatment at the University of Tokyo Hospital as approved by the Institutional Review Board. Tumors were washed, and mechanically and enzymatically dissociated into single cells. Tumor cells were cultured in Neurobasal medium (Life Technologies, Carlsbad, CA, USA) containing B27 supplement minus vitamin A (Life Technologies), epidermal growth factor and basic fibroblast growth factor (20 ng/ml each; Wako Pure Chemical Industries, Osaka, Japan). For *in vitro* differentiation, tumor cells were cultured in Dulbecco's modified Eagle's medium/F-12 medium (Life Technologies) containing 10% fetal bovine serum. Cell viability was assessed using the CellTiter-Glo Luminescent Cell Viability Assay (Promega, Madison, WI, USA).

Antibodies

Mouse monoclonal antibodies to cyclin B1, E2F1 and α-tubulin were obtained from Santa Cruz Biotechnology (Santa Cruz, CA, USA). Mouse monoclonal antibodies to cyclin D1, D2, D3 and RB were from BD Biosciences (Billerica, MA, USA). Mouse monoclonal antibody to glyceraldehyde-3-phosphate dehydrogenase (GAPDH) was from Millipore (Bedford, MA, USA). Rabbit polyclonal antibodies to E2F2 and green fluorescence protein (GFP) were from Santa Cruz Biotechnology. Rabbit pAbs to phospho-RB S780, S795 and S807/811 were from Cell Signaling Technology (Danvers, MA, USA).

Immunoblotting

Cells were lysed in lysis buffer (50 mM Tris-HCl, pH 7.5, 250 mM NaCl, 0.1% Triton X-100, 1 mM dithiothreitol, 1 mM EDTA, 50 mM NaF, 0.1 mM Na_3VO_4 and protease inhibitors). Lysates were fractionated by sodium dodecyl sulfate–polyacrylamide gel electrophoresis and transferred to a polyvinylidene difluoride membrane (Immobilon-P; Millipore). The membrane was subjected to immunoblot analysis using horseradish peroxidase-conjugated donkey anti-rabbit immunoglobulin G (GE Healthcare, Pittsburgh, PA, USA) or sheep anti-mouse immunoglobulin G (GE Healthcare) as a secondary antibody. Visualization was performed using the Enhanced Chemiluminescence Plus Western Blotting Detection System (GE Healthcare) and LAS-4000EPUVmini Luminescent Image Analyzer (GE Healthcare).

Quantitative RT–PCR

Total RNA was extracted using NucleoSpin RNA Clean-up kit (Takara Bio Inc., Shiga, Japan) and reverse-transcribed into cDNA using ReverTra Ace qPCR RT Kit (Toyobo Life Science, Osaka, Japan). Real-time PCR was performed using LightCycler480 SYBR Green I Master and a LightCycler480 Instrument (Roche, Indianapolis, IN, USA). The results were normalized with the detected value for *GAPDH* or *ACTB*. Primers used in RT–PCR were as follows: *GAPDH* forward (5′-GCACCGTCAAGGCTGAGAAC-3′), *GAPDH* reverse (5′-TGGTGAAGACGCCAGTGGA-3′); *CD133* forward (5′-AGTGG CATCGTGCAAACCTG-3′), *CD133* reverse (5′-CTCCGAATCCATTCGACGA TAGTA-3′); *nestin* forward (5′-GAGGTGGCCACGTACAGG-3′), *nestin* reverse (5′-AAGCTGAGGGAAGTCTTGGA-3′); *cyclin D1* forward (5′-TGTCCTACT ACCGCCTCACA-3′), *cyclin D1* reverse (5′-CAGGGCTTCGATCTGCTC-3′); *cyclin D2* forward (5′-GGACATCCAACCCTACATGC-3′), *cyclin D2* reverse (5′-CGCACTTCTGTTCCTCACAG-3′); and *cyclin D3* forward (5′-GCTTAC TGGATGCTGGAGGTA-3′), *cyclin D3* reverse (5′-AAGACAGGTAGCGATCCAG GT-3′). Human-specific primers were as follows: *ACTB* forward (5′-CGTCACC AACTGGGACGACA-3′), *ACTB* reverse (5′-CTTCTCGCGGTTGGCCTTGG-3′); *cyclin D1* forward (5′-ACTACCGCCTCACACGCTTC-3′), *cyclin D1* reverse (5′-CTTGACTCCAGCAGGGCTTC-3′); *cyclin D2* forward (5′-ATCACCAACAC AGACGTGGA-3′), *cyclin D2* reverse (5′-TGCAGGCTATTGAGGAGCA-3′); and *cyclin D3* forward (5′-TACACCGACCACGCTGTCT-3′), *cyclin D3* reverse (5′-GAAGGCCAGGAAATCATGTG-3′). Mouse-specific primers were as follows: *ACTB* forward (5′-GGATGCAGAAGGAGATTACTGC-3′), *ACTB* reverse (5′-CCACCGATCCACACAGAGCA-3′).

RNA interference

The stealth siRNA oligonucleotide sequences were 5′-CCACAGAUGUGAA GUUCAUUUCCAA-3′ (cyclin D1), 5′-UGCUCCUCAAUAGCCUGCAGCAGUA-3′ (cyclin D2#1), 5′-UGACGGAUCCAAGUCGGAGGAUGAA-3′ (cyclin D2#2), 5′-AACUACCUGGAUCGCUACCUGUCUU-3′ (cyclin D3), 5′-GGGAGAUCA AGGUAACCCUGGUGUU-3′ (CDK4) and 5′-ACCGAGUAGUGCAUCGCGAU CUAAA-3′ (CDK6) (Life Technologies). Negative control stealth siRNA with medium GC content was purchased from Life Technologies. The silencer select siRNA oligonucleotide sequences were 5′-GGACCUUCGUAGCAUUG CATT-3′ (E2F1) and 5′-AGACAGUGAUUGCCGUCAATT-3′ (E2F2) (Life Technologies). Negative control silencer select siRNA was purchased from Life Technologies. Transfection of siRNA was performed using Lipofectamine RNAiMAX transfection reagent (Life Technologies). shRNAs targeting cyclin D2 were designed to harbor the same target sequences.

Flow cytometry

Cells were trypsinized, fixed in 70% ethanol and then stained with propidium iodide (Sigma, St Louis, MO, USA). Cells were passed through a FACSCalibur instrument (BD Biosciences) and the data were analyzed using the ModFit LT software (Verity Software House, Topsham, ME, USA).

Lentivirus production

Lentiviral vector CS-RfA-CG harboring an shRNA driven by the H1 promoter or CSII-CMV-RfA-IRES2-Venus harboring a cDNA driven by the CMV promoter was transfected with the packaging vectors pCAG-HIV-gp and pCMV-VSV-G-RSV-Rev into 293FT cells using Lipofectamine 2000 Transfection Reagent (Life Technologies). All plasmids were kindly provided by H

Miyoshi (RIKEN BioResource Center, Ibaraki, Japan). Viral supernatant was purified by ultracentrifugation at 25 000 r.p.m. for 90 min (SW28 rotor, Beckman Coulter, Brea, CA, USA). Infection efficiency was monitored by GFP expression as it is driven by the CMV promoter.

Intracranial xenografts

At 1 week after lentivirus infection, 1×10^4 cells were injected stereotactically into the right frontal lobe of 5-week-old nude mice (BALB/cAJcl-*nu/nu*; CLEA Japn Inc., Tokyo, Japan), following administration of general anesthesia ($n = 6$). The injection coordinates were 2 mm to the right of the midline, 1 mm anterior to the coronal suture and 3 mm deep. Mice were monitored for 6 months. Survival of mice was evaluated by Kaplan–Meier analysis. *P*-value was calculated using a log-rank test. Tumors were histologically analyzed after hematoxylin and eosin staining. Tumor distribution was analyzed by GFP immunostaining. All animal experimental protocols were performed in accordance with the politics of the Animal Ethics Committee of the University of Tokyo.

Immunohistochemistry

Samples were fixed in 3.7% buffered formalin, dehydrated and embedded in paraffin. Sections (6 μm) were rehydrated, and endogenous peroxidases were blocked by incubation in 0.3% H_2O_2 for 30 min. The primary antibody was detected using the VECTASTAIN ABC kit (Vector Laboratories, Burlingame, CA, USA). Slides were lightly counterstained with hematoxylin.

Microarray data

The expression profiles of undifferentiated GB1–3 and 5 cells were generated on the Affymetrix GeneChip HG-U133 Plus 2.0 microarray platform (Affymetrix, Santa Clara, CA, USA). The expression profiles of 15 GSCs were taken from the Gene Expression Omnibus database GSE7181 and GSE8049 (Lottaz *et al.*[9]).Data were analyzed using the software program GenePattern. The expression profiles of D-type cyclins in various histological grades of glioma were taken from GSE4290 (Sun *et al.*[17]). Data were analyzed using the software program R. *P*-value was calculated using a pairwise Wilcoxon's test. The expression profiles of D-type cyclins in patient glioblastomas, glioma cell lines and normal NSCs were taken from GSE4536 (Lee *et al.*[4]).

CONFLICT OF INTEREST

The authors declare no conflict of interest.

ACKNOWLEDGEMENTS

This work was supported by Research Program of Innovative Cell Biology by Innovative Technology (Integrated Systems Analysis of Cellular Oncogenic Signaling Networks), Grants-in-Aid for Scientific Research on Innovative Areas (Integrative Research on Cancer Microenvironment Network), Takeda Science Foundation and in part by Global COE Program (Integrative Life Science Based on the Study of Biosignaling Mechanisms), MEXT, Japan.

REFERENCES

1 Furnari FB, Fenton T, Bachoo RM, Mukasa A, Stommel JM, Stegh A *et al.* Malignant astrocytic glioma: genetics, biology, and paths to treatment. *Genes Dev* 2007; **21**: 2683–2710.
2 Alison MR, Lim SM, Nicholson LJ. Cancer stem cells: problems for therapy? *J Pathol* 2011; **223**: 147–161.
3 Singh SK, Clarke ID, Terasaki M, Bonn VE, Hawkins C, Squire J *et al.* Identification of a cancer stem cell in human brain tumors. *Cancer Res* 2003; **63**: 5821–5828.
4 Lee J, Kotliarova S, Kotliarov Y, Li A, Su Q, Donin NM *et al.* Tumor stem cells derived from glioblastomas cultured in bFGF and EGF more closely mirror the phenotype and genotype of primary tumors than do serum-cultured cell lines. *Cancer Cell* 2006; **9**: 391–403.
5 Sherr CJ, Roberts JM. Living with or without cyclins and cyclin-dependent kinases. *Genes Dev* 2004; **18**: 2699–2711.
6 Sherr CJ, McCormick F. The RB and p53 pathways in cancer. *Cancer Cell* 2002; **2**: 103–112.
7 Cancer Genome Atlas Research Network. Comprehensive genomic characterization defines human glioblastoma genes and core pathways. *Nature* 2008; **455**: 1061–1068.
8 Parsons DW, Jones S, Zhang X, Lin JC, Leary RJ, Angenendt P *et al.* An integrated genomic analysis of human glioblastoma multiforme. *Science* 2008; **321**: 1807–1812.
9 Lottaz C, Beier D, Meyer K, Kumar P, Hermann A, Schwarz J *et al.* Transcriptional profiles of CD133 + and CD133 − glioblastoma-derived cancer stem cell lines suggest different cells of origin. *Cancer Res* 2010; **70**: 2030–2040.
10 Mizrak D, Brittan M, Alison MR. CD133: molecule of the moment. *J Pathol* 2008; **214**: 3–9.
11 Lendahl U, Zimmerman LB, McKay RD. CNS stem cells express a new class of intermediate filament protein. *Cell* 1990; **60**: 585–595.
12 Sanai N, Alvarez-Buylla A, Berger MS. Neural stem cells and the origin of gliomas. *N Engl J Med* 2005; **353**: 811–822.
13 Kowalczyk A, Filipkowski RK, Rylski M, Wilczynski GM, Konopacki FA, Jaworski J *et al.* The critical role of cyclin D2 in adult neurogenesis. *J Cell Biol* 2004; **167**: 209–213.
14 Walzlein JH, Synowitz M, Engels B, Markovic DS, Gabrusiewicz K, Nikolaev E *et al.* The antitumorigenic response of neural precursors depends on subventricular proliferation and age. *Stem Cells* 2008; **26**: 2945–2954.
15 Mayr C, Bartel DP. Widespread shortening of 3'UTRs by alternative cleavage and polyadenylation activates oncogenes in cancer cells. *Cell* 2009; **138**: 673–684.
16 Zhang X, Zhao M, Huang AY, Fei Z, Zhang W, Wang XL. The effect of cyclin D expression on cell proliferation in human gliomas. *J Clin Neurosci* 2005; **12**: 166–168.
17 Sun L, Hui AM, Su Q, Vortmeyer A, Kotliarov Y, Pastorino S *et al.* Neuronal and glioma-derived stem cell factor induces angiogenesis within the brain. *Cancer Cell* 2006; **9**: 287–300.

Supplementary Information accompanies the paper on the Oncogene website (http://www.nature.com/onc)

IJC
International Journal of Cancer

An armed oncolytic herpes simplex virus expressing thrombospondin-1 has an enhanced *in vivo* antitumor effect against human gastric cancer

Toshiaki Tsuji[1], Mikihito Nakamori[1], Makoto Iwahashi[1], Masaki Nakamura[1], Toshiyasu Ojima[1], Takeshi Iida[1], Masahiro Katsuda[1], Keiji Hayata[1], Yasushi Ino[2], Tomoki Todo[2] and Hiroki Yamaue[1]

[1] Second Department of Surgery, Wakayama Medical University School of Medicine, 811-1 Kimiidera, Wakayama 641-8510, Japan
[2] Division of Innovative Cancer Therapy, The advanced Clinical Research Center, The Institute of Medical Science, The University of Tokyo, 4-6-1 Shirokanedai, Minato-ku, Tokyo 108-8639, Japan

Advanced gastric cancer is a common disease, but the conventional treatments are unsatisfactory because of the high recurrence rate. One of the promising new therapies is oncolytic virotherapy, using oncolytic herpes simplex viruses (HSVs). Thrombospondin-1 (TSP-1) suppresses tumor progression *via* multiple mechanisms including antiangiogenesis. Our approach to enhance the effects of oncolytic HSVs is to generate an armed oncolytic HSV that combines the direct viral oncolysis with TSP-1-mediated function for gastric cancer treatment. Using the bacterial artificial chromosome (BAC) system, a 3rd generation oncolytic HSV (T-TSP-1) expressing human TSP-1 was constructed for human gastric cancer treatment. The enhanced efficacy of T-TSP-1 was determined in both human gastric cancer cell lines *in vitro* and subcutaneous tumor xenografts of human gastric cancer cells *in vivo*. In addition, we examined the apoptotic effect of T-TSP-1 *in vitro*, and the antiangiogenic effect of T-TSP-1 *in vivo* compared with a non-armed 3rd generation oncolytic HSV, T-01. No apparent apoptotic induction by T-TSP-1 was observed for human gastric cancer cell lines TMK-1 cells but for MKN1 cells *in vitro*. Arming the viruses with TSP-1 slightly inhibited their replication in some gastric cancer cell lines, but the viral cytotoxicity was not attenuated. In addition, T-TSP-1 exhibited enhanced therapeutic efficacy and inhibition of angiogenesis compared with T-01 *in vivo*. In this study, we established a novel armed oncolytic HSV, T-TSP-1, which enhanced the antitumor efficacy by providing a combination of direct viral oncolysis with antiangiogenesis. Arming oncolytic HSVs may be a useful therapeutic strategy for gastric cancer therapy.

Gastric cancer currently ranks second in global cancer mortality.[1,2] Most patients are diagnosed at an advanced stage and curative surgical treatments are sometimes difficult due to the presence of peritoneal dissemination or extra-regional lymph node metastases. The long-term prognosis of curatively resected advanced gastric cancer remains unsatisfactory because of its high recurrence rate after surgery. The available chemotherapeutic reagents have only limited efficacy against these recurrent diseases. Therefore, new therapeutic strategies for advanced and recurrent gastric cancers are urgently needed.

Key words: oncolytic virus, herpes simplex virus, thrombospondin-1, gastric cancer, antiangiogenesis
Grant sponsor: Japan Society for the Promotion of Science (JSPS) Grants-in Aid for Scientific Research; Grant numbers: 17591433, 20591574; Grant sponsor: Takeda Science Foundation, Japan
DOI: 10.1002/ijc.27681
History: Received 16 Jan 2012; Accepted 1 Jun 2012; Online 22 Jun 2012
Correspondence to: Mikihito Nakamori, Second Department of Surgery, Wakayama Medical University, School of Medicine, 811-1 Kimiidera, Wakayama 641-8510, Japan, Tel.: +81-73-441-0613, Fax: +81-73-446-6566, E-mail: chamcham@wakayama-med.ac.jp

Replication-selective oncolytic herpes simplex viruses (HSVs) have emerged as a new platform for cancer therapy. Several oncolytic HSV mutants (1716, G207, NV1020 and OncoVex$^{GM\text{-}CSF}$) have already entered Phase I, II and III clinical trials for various solid tumors.[3–7] Despite the significant efficacy in preclinical models and safety in humans, however, the therapeutic benefits appear to be limited in cancer patients. It is therefore prudent to incorporate mechanisms in addition to direct oncolysis to enhance the tumor cell destruction. To this end, we have already shown that oncolytic HSVs with membrane fusion activity resulting from either genetically inserting a hyperfusogenic glycoprotein or random mutagenesis have an enhanced antitumor potency, while also exerting a synergistic effect on syncytial formation which facilitates the spread of the oncolytic virus in tumor tissue.[8–10] In addition, our collaborators have previously shown that HSV mutant G47Δ, in addition to enhanced viral replication, also possesses an immunoregulatory function, by which MHC Class I presentation was increased compared with its parent virus, G207, while maintaining the safety profile of G207.[11] This provides for the possibility of developing an enhanced cytotoxic lymphocyte response toward tumor cells and increased efficacy of the virus.

What's new?

Oncolytic virotherapy using herpes simplex virus (HSV) engineered to destroy tumor cells represents a promising new anticancer strategy. In this study, to enhance the effects of oncolytic HSV, an "armed" virus expressing human thrombospondin-1 (TSP-1), an antiangiogenic protein, was developed. The armed virus, T-TSP-1, inhibited human gastric cancer cell growth both *in vitro* and *in vivo*. The enhanced viral antitumor efficacy observed suggests that T-TSP-1 may be a useful tool in the treatment of gastric cancer.

Another problem with oncolytic virotherapy is the rapid innate immune responses that accompany viral infection, which induces the upregulation of angiogenic factors, such as vascular endothelial growth factor, and the downregulation of antiangiogenic factors, such as thrombospondin-1 (TSP-1) and thrombospondin-2 (TSP-2).[12,13] Moreover, Aghi *et al.* reported that TSP-1 reduction, accompanied with oncolytic virotherapy, induced increased angiogenesis of the residual tumor and resulted in the regrowth of tumors after oncolytic virotherapy.[12]

TSP-1 is a multifunctional 450 kDa homotrimetric glycoprotein and was originally described as a naturally occurring antiangiogenic factor and later as a potent tumor inhibitor.[14–16] The antitumor mechanisms of TSP-1 are reported to include antiangiogenesis *via* CD36,[17] induction of apoptosis,[18,19] latent transforming growth factor β (TGF-β) activation[20] and inhibition of matrix metalloproteinase 9 (MMP-9) activation.[21] TSP-1 mimetics and genes expressing them have been reported to have synergism when used with oncolytic HSV[12,22] and chemotherapeutic reagents, such as paclitaxel and cisplatin.[23] While TSP-1 is expected to have various effects that could be useful for cancer therapy, its use in infusion or injection treatments is limited because of its size and difficulty in large-scale production, and non-viral and replication-deficient viral vectors are thought to have limited success due to their poor distribution in the solid tumor mass and the tumor microenvironment.

To resolve these problems, we used replication-competent oncolytic HSVs as a vector to deliver TSP-1 to a tumor and its microenvironment, and hypothesized that, if oncolytic HSVs were combined with TSP-1, they would exert enhanced antitumor efficacy. Our viruses showed enhanced antitumor effects both *in vitro* and *in vivo via* direct antitumor and antiangiogenic mechanisms.

Material and Methods

Cell lines and viruses

Vero (Africa green monkey kidney), AZ521, MKN1, MKN28, MKN45 and MKN74 (human gastric cancer cell lines) cells were originally obtained from the RIKEN BioResource Center (Tsukuba, Japan). All of the cell lines were authenticated according to the Cell Line Verification Test Recommendations of ATCC Technical Bulletin no.8 (2008) within 3 months. TMK-1 cells, a human gastric cancer cell line, were a gift from Dr. Eiichi Tahara (Hiroshima University, Hiroshima, Japan). The TMK-1, MKN1, MKN28, MKN45 and MKN74 cells were cultured in RPMI1640 containing 10% fetal bovine serum (FBS) (GIBCO, Grand Island, NY). AZ521 cells and Vero cells were cultured in dulbecco's modified eagle medium (DMEM) containing 10% FBS. T-01 is an HSV-1-based oncolytic virus, constructed by deleting the ICP6 gene, α47 gene and both copies of the γ34.5 gene. The details of its construction have been published previously.[11] Viral stocks were prepared by releasing the virus from infected Vero cells with heparin, followed by high-speed centrifugation, as described previously.[8]

Cloning of thrombospondin-1 cDNA

Total RNA was extracted from normal human blood cells using an RNA Blood mini kit (Qiagen, Hilden, Germany), and reverse transcription PCR amplification with ReverTra Ace-α (Toyobo, Osaka, Japan). TSP-1 cDNA PCR amplification was performed with KOD plus (Toyobo). The oligonucleotide primer sequences used were follows: 5′-TA CAC ACA GGA TCC CTG CT-3′, sense, and 5′-TTA GGG ATC TCT ACA TTC GTA TTT CA-3′, antisense, for TSP-1 cDNA. The obtained human TSP-1 cDNA fragment was cloned into a cloning site of the pTA2 vector, named pTA2-TSP-1, using a TArget Clone Plus kit (Toyobo) according to the manufacturer's instructions. The sequence of obtained pTA2-TSP-1 was compared with the GenBank sequence of human TSP-1 (accession no. NM_003246) and confirmed. A 3.7-kb *EcoRV-SacII* fragment containing a human TSP-1 cDNA fragment was inserted into the *StuI-SacII* site of SV-01 to generate SV-TSP-1.

Construction of the virus

Using a bacterial artificial chromosome (BAC) and Cre/loxP and FLPe/FRT recombinase systems, oncolytic HSVs were constructed. Mutagenesis of the T-BAC plasmid was done by a two-step replacement procedure as reported in a previous study.[24,25] The T-BAC plasmid (1.5 μg) and SV-TSP-1 (150 ng) were mixed and incubated with Cre recombinase (New England BioLabs, Ipswich, MA) and were electroporated into *E. coli* ElectroMaxDH10B (Invitrogen, Carlsbad, CA) using a Gene Pulser (Bio-Rad Laboratories, Hercules, CA). The bacteria were streaked onto LB plates containing Cm (15 μg/ml) and Kan (10 μg/ml) and incubated to select clones containing the mutant BAC plasmid. Recombinant T-BAC/SV-TSP-1 was digested with *Hind* III and electrophoresed on a 0.8% SeaKem GTG Agarose Gel (Takara Bio, Shiga, Japan) in TAE buffer at 2.5 cm/V for 18 hr with High MW DNA Markers